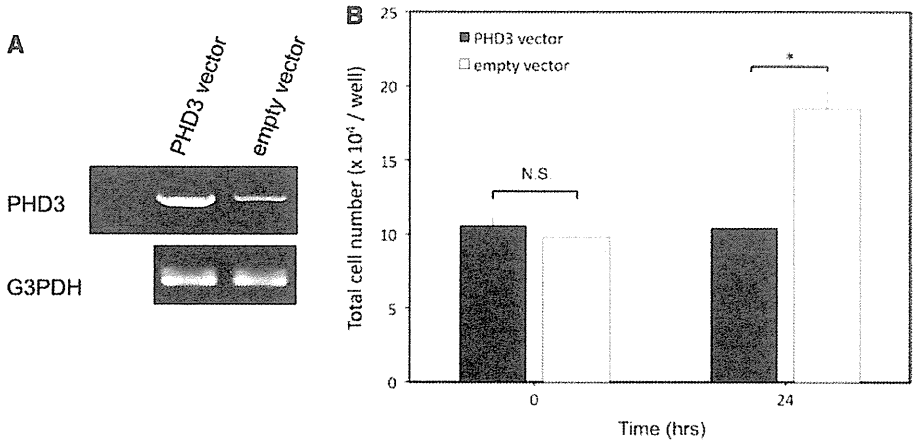

Fig. 5 In vitro deterioration of cell proliferation by gene transfection of PHD3. **a** RT-PCR revealed that PHD3 was overexpressed in ACHN transfected with the PHD3 plasmid compared with an empty vector. **b** Cell number was significantly decreased in ACHN with the PHD3 plasmid compared with the empty vector. Data are shown as mean ± SEM of three independent experiments. *$p < 0.005$

PHD3 expression is an independent predictor of prolonged recurrence-free survival in CCRCC

Patients and tumor characteristics are shown in Table 1. PHD3-positive cells were observed in 82 (70.7 %) of the 116 cases (Fig. 6). The 5-year RFS rates were 90.8 and 69.9 % in patients with PHD3-positive and PHD3-negative tumors, respectively ($p = 0.0032$), although there was no significant difference in CSS between the 2 groups (Fig. 7). Multivariate analysis revealed that PHD3 expression was an independent predictor of favorable RFS when adjusted for known prognostic factors such as the pathological stage and Fuhrman grade (Table 2).

Table 1 Characteristics of the 116 patients

Characteristics	
Median age in years (range)	60 (28–85)
Median follow-up (months)	64
Sex	
Male	92 (79.3)
Female	24 (20.7)
ECOG PS	
0	102 (76.7)
1	27 (20.3)
2	3 (2.2)
3	1 (0.8)
Clinical stage	
Stage I	72 (54.1)
Stage II	9 (6.8)
Stage III	31 (23.3)
Stage IV	21 (15.8)
Fuhrman grade	
Grade 1	45 (33.8)
Grade 2	69 (51.9)
Grade 3	19 (14.3)
Grade 4	0 (0)

Values are *N* (%) except where indicated otherwise

Discussion

HIF was first identified as a regulator of hypoxia-induced erythropoietin expression (Semenza and Wang 1992; Wang et al. 1995; Wang and Semenza 1995). HIF-1α and HIF-2α are important regulators of tumor progression that induce more than 60 growth factors such as VEGF, platelet-derived growth factor, insulin-like growth factor, fibroblast growth factor and so on (Maynard and Ohh 2007). PHDs hydroxylate two conserved proline residues of HIF-1α and HIF-2α, leading to capture by the corresponding E3 ubiquitin–ligase VHL complex and degradation under normoxia, and lose the activity under hypoxia (Bruick and McKnight 2001; Cockman et al. 2000; Ivan et al. 2001; Jaakkola et al. 2001; Yu et al. 2001). As a result, PHDs control the activities of HIF protein under normoxic conditions. Therefore, it is considered that HIF-1α and HIF-2α can act only in a hypoxic microenvironment or cells with inactivated VHL protein.

The present study demonstrated two different mechanisms of PHD3 expression in RCCs that were observed under normoxia. RCC cell lines with VHL gene mutation had high expression of PHD3 under normoxia. This expression might be a feedback reaction from stable HIF protein accumulation. The mechanism possibly applies to CCRCC, which accounts for a large portion of RCCs (Aprelikova et al. 2004; Marxsen et al. 2004; Maxwell et al. 1999; Shinojima et al. 2007). Interestingly, normoxic expression of PHD3, which is regulated by a signal transduction pathway, could be seen in VHL-intact cells. Although the PI3 K/Akt pathway is a known regulator of HIF-1α expression (Blancher et al. 2001; Brugarolas et al. 2003; Hudson et al. 2002; Laughner et al. 2001; Pore et al. 2006; Zhong et al.

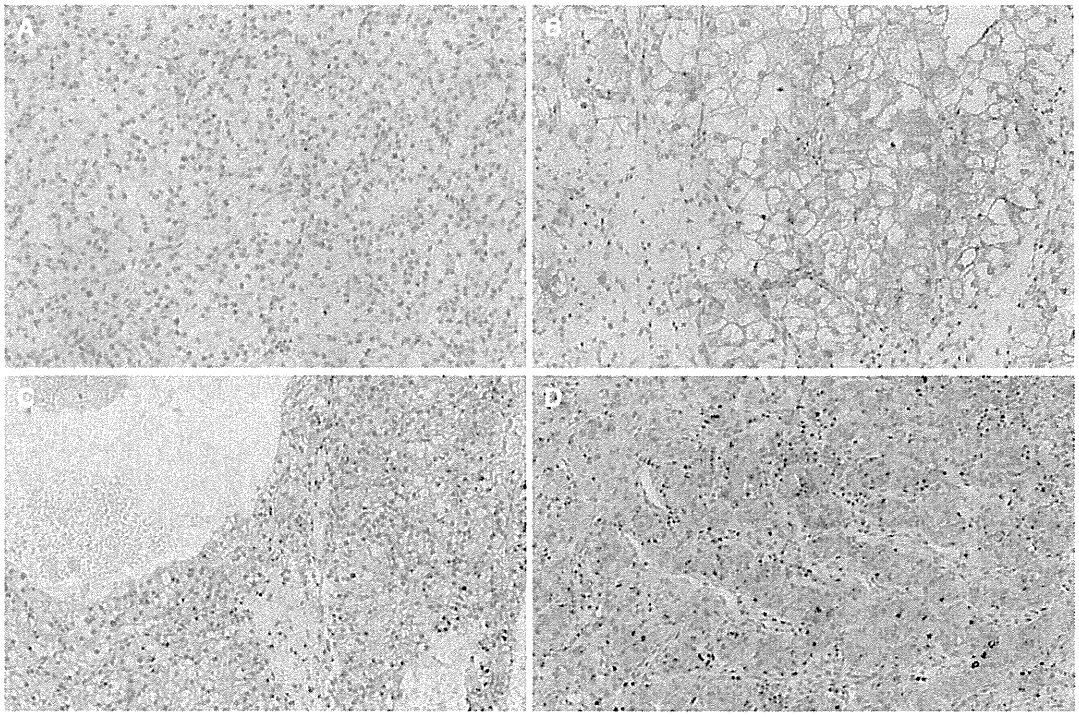

Fig. 6 Representative immunohistochemical staining of PHD3 in tumor tissue section of clear cell renal cell carcinoma. **a** Negative PHD3 expression in tumor cells. **b–d** Positive PHD3 expression in tumor cells

1998), we found that activation of the PI3K/Akt/mTOR pathway induced PHD3 expression irrespective of HIF protein accumulation. To the best of our knowledge, there has been no report proving an HIF-independent mechanism of PHD3 expression.

In this study, PHD3 silencing promoted proliferation of VHL-intact cells, although it did not induce HIF proteins accumulation, unlike PHD2 (Berra et al. 2003). Moreover, PHD3 silencing also promoted cell proliferation also in VHL-mutant cell lines, where HIF proteins were stably accumulated irrespective of hydroxylation. These results suggested that PHD3 had a direct antiproliferative function that was independent of HIF proteins and the VHL gene status in RCCs. In neuronal cells, PHD3 is induced after withdraw of nerve growth factor and promotes apoptosis (Lipscomb et al. 1999, 2001; Straub et al. 2003). However, this function is dependent on HIF-hydroxylase activity (Lee et al. 2005). Su et al. reported that PHD3 induced apoptosis independently of HIF-1 in pancreatic cancer (Su et al. 2010). In their report, the expression was induced and the apoptotic function enhanced under hypoxia. Our findings were in accord with their results in terms of the HIF-independent antiproliferative function. Moreover, our results suggested that PHD3 was expressed and suppressed cancer cell proliferation under normoxia in RCC, although this study has some limitations. The major one is that PHD3 expression was evaluated only by the mRNA level, not by the protein level in vitro, and the expression of mRNA does not always correlate with that of protein. In addition, we could not verify the expression mechanism and function of PHD3 in vivo because we could not obtain stable transfectants of cell lines with siRNA and the PHD3 gene. Although further investigation is needed to clarify the detailed mechanisms, results of the current study suggested that PHD3 was a potential antitumor molecule, which could be employed for gene or molecule target therapy irrespective of the VHL and HIF status and tissue oxygenic condition.

The results of the immunohistochemical study of PHD3 expression using primary tissue of CCRCC supported the view shown by the in vitro study, though the follow-up duration may have be insufficient to prove an impact on CSS, unlike RFS in this series. The expression of HIF-1α and -2α was not evaluated by immunohistochemistry in the present study. HIF protein expression should have been evaluated to indicate the concordance with the results of the in vitro study. However, the methods for evaluation of the expression are different among reports. Furthermore, positive rates of HIF-1α and HIF-2α also differ, ranging from 37–83 to 82–95 %, respectively (Atkins et al. 2005; Gordan et al. 2008; Klatte et al. 2007; Kroeze et al. 2010; Ku et al. 2011). Thus, it may be difficult to determine the association

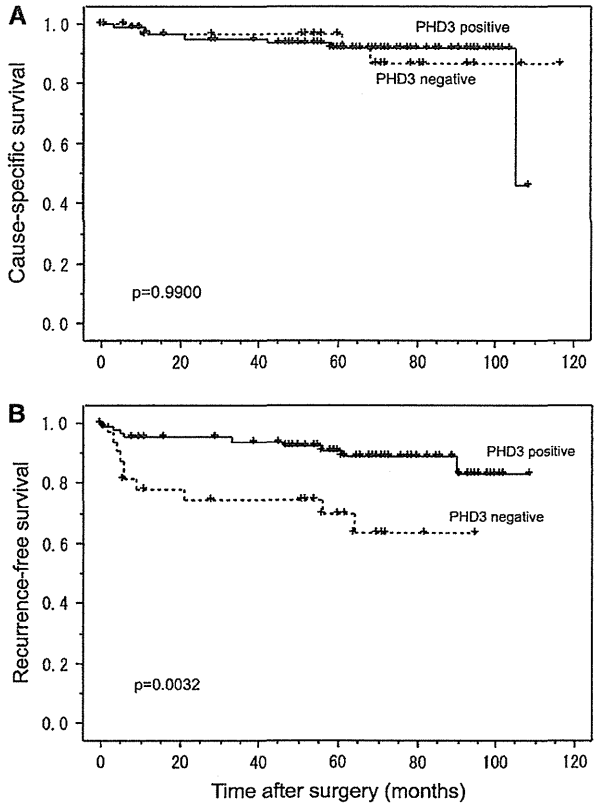

Fig. 7 Kaplan–Meier curves for cancer-specific survival (**a**) and recurrence-free survival (**b**) according to PHD3 status

Table 2 Prognostic factors for recurrence-free survival in univariate and multivariate analyses

	Univariate[a]		Multivariate[b]	
Factor	*n*	*p* value	*p* value	HR (95 % CI)
PHD3 positive	82	0.0032	0.0463	0.361 (0.133–0.983)
Fuhrman grade 3	12	0.0022	0.0365	3.331 (1.079–10.286)
Stage III or more	35	<0.0001	0.0042	4.837 (1.646–14.215)
Age >50 years	93	0.0852	0.4624	2.175 (0.274–17.274)
Female gender	24	0.9306	0.9795	1.015 (0.323–3.188)

HR hazard ratio, *CI* confidence interval

[a] Performed by using the log-rank test

[b] Done by using the Cox proportional hazard regression models

between the expression of PHD3 and that of HIF proteins by immunohistochemistry.

It is still unclear why PHD3, which can be induced through proliferative signals, has a paradoxical antiproliferative function. We speculate that PHD3 may play a role as a checkpoint mechanism in RCC cells that controls their growth and metabolites to adapt to the tissue environment. Commonly, CCRCC is known as a slow-growing tumor, and the majority of cases of CCRCC are discovered in the early stage and associated with a favorable prognosis (Volpe and Jewett 2005). High PHD3 expression may be consistent with this clinical feature. On the other hand, a few CCRCCs grow rapidly and are associated with poor prognosis. In some of these cases, a disturbance of PHD3 expression due to gene mutation or epigenetic processes may promote cell proliferation and correlate with tumor aggressiveness. To clarify this issue, further investigation is needed.

Conclusions

The results of the current study demonstrate that PHD3 expression can be induced in VHL-intact RCCs under normoxia via activation of the PI3 K/Akt/mTOR pathway independently of HIF-1α and HIF-2α. In addition, PHD3 has an antiproliferative function that is independent of HIF and VHL gene status. These findings reveal a novel expression mechanism and function of PHD3 in RCC.

Acknowledgments We thank Emiri Nakazawa, Akari Takahashi and Eri Saka for their skillful technical assistance, and Mr. Kim Barrymore for English correction of this manuscript. This study was supported in part by a grant-aid from Ministry of Education, Culture, Sports, Science and Technology of Japan.

Conflict of interest All authors of this paper reported no financial interests or potential conflict of interests.

References

Appelhoff RJ, Tian YM, Raval RR, Turley H, Harris AL, Pugh CW, Ratcliffe PJ, Gleadle JM (2004) Differential function of the prolyl hydroxylases PHD1, PHD2, and PHD3 in the regulation of hypoxia-inducible factor. J Biol Chem 279:38458–38465

Aprelikova O, Chandramouli GV, Wood M, Vasselli JR, Riss J, Maranchie JK, Linehan WM, Barrett JC (2004) Regulation of HIF prolyl hydroxylases by hypoxia-inducible factors. J Cell Biochem 92:491–501

Atkins DJ, Gingert C, Justenhoven C, Schmahl GE, Bonato MS, Brauch H, Störkel S (2005) Concomitant deregulation of HIF1a and cell cycle proteins in VHL-mutated renal cell carcinomas. Virchows Arch 447:634–642

Berra E, Benizri E, Ginouves A, Volmat V, Roux D, Pouyssegur J (2003) HIF prolyl-hydroxylase 2 is the key oxygen sensor setting low steady-state levels of HIF-1a in normoxia. EMBO J 22:4082–4090

Blancher C, Moore JW, Robertson N, Harris AL (2001) Effects of ras and von Hippel-Lindau (VHL) gene mutations on hypoxia-inducible factor (HIF)-1α, HIF-2α, and vascular endothelial growth factor expression and their regulation by the phosphatidylinositol 3′-kinase/Akt signaling pathway. Cancer Res 61:7349–7355

Brugarolas JB, Vazquez F, Reddy A, Sellers WR, Kaelin WG Jr (2003) TSC2 regulates VEGF through mTOR-dependent and -independent pathways. Cancer Cell 4:147–158

Bruick RK, McKnight SL (2001) A conserved family of prolyl-4-hydroxylases that modify HIF. Science 294:1337–1340

Cioffi CL, Liu XQ, Kosinski PA, Garay M, Bowen BR (2003) Differential regulation of HIF-1α prolyl-4-hydroxylase genes by hypoxia in human cardiovascular cells. Biochem Biophys Res Commun 303:947–953

Cockman ME, Masson N, Mole DR, Jaakkola P, Chang GW, Clifford SC, Maher ER, Pugh CW, Ratcliffe PJ, Maxwell PH (2000) Hypoxia inducible factor-a binding and ubiquitylation by the von Hippel-Lindau tumor suppressor protein. J Biol Chem 275:25733–25741

del Peso L, Castellanos MC, Temes E, Martin-Puig S, Cuevas Y, Olmos G, Landazuri MO (2003) The von Hippel Lindau/hypoxia-inducible factor (HIF) pathway regulates the transcription of the HIF-proline hydroxylase genes in response to low oxygen. J Biol Chem 278:48690–48695

Edge SB, Byrd DR, Compton CC, Fritz AG, Greene FL, Trotti A (2010) American Joint Committee on Cancer (AJCC) staging manual, 7th edn. Springer, Philadelphia

Fuhrman S, Lasky LC, Limas L (1982) Prognostic significance of morphologic parameters in renal cell carcinoma. Am J Surg Pathol 6:655

Gordan JD, Lal P, Dondeti VR, Letrero R, Parekh KN, Oquendo CE, Greenberg RA, Flaherty KT, Rathmell WK, Keith B, Simon MC, Nathanson KL (2008) HIF-α effects on c-Myc distinguish two subtypes of sporadic VHL-deficient clear cell renal carcinoma. Cancer Cell 14:435–446

Hirsila M, Koivunen P, Gunzler V, Kivirikko KI, Myllyharju J (2003) Characterization of the human prolyl 4-hydroxylases that modify the hypoxia-inducible factor. J Biol Chem 278:30772–30780

Huang J, Zhao Q, Mooney SM, Lee FS (2002) Sequence determinants in hypoxia-inducible factor-1a for hydroxylation by the prolyl hydroxylases PHD1, PHD2, and PHD3. J Biol Chem 277:39792–39800

Hudson CC, Liu M, Chiang GG, Otterness DM, Loomis DC, Kaper F, Giaccia AJ, Abraham RT (2002) Regulation of hypoxia-inducible factor 1a expression and function by the mammalian target of rapamycin. Mol Cell Biol 22:7004–7014

Ivan M, Kondo K, Yang H, Kim W, Valiando J, Ohh M, Salic A, Asara JM, Lane WS, Kaelin WG Jr (2001) HIFα targeted for VHL-mediated destruction by proline hydroxylation: implications for O2 sensing. Science 292:464–468

Jaakkola P, Mole DR, Tian YM, Wilson MI, Gielbert J, Gaskell SJ, von Kriegsheim A, Hebestreit HF, Mukherji M, Schofield CJ, Maxwell PH, Pugh CW, Ratcliffe PJ (2001) Targeting of HIF-α to the von Hippel-Lindau ubiquitylation complex by O2-regulated prolyl hydroxylation. Science 292:468–472

Klatte T, Seligson DB, Riggs SB, Leppert JT, Berkman MK, Kleid MD, Yu H, Kabbinavar FF, Pantuck AJ, Belldegrun AS (2007) Hypoxia-inducible factor 1α in clear cell renal cell carcinoma. Clin Cancer Res 13:7388–7393

Kroeze SG, Vermaat JS, van Brussel A, van Melick HH, Voest EE, Jonges TG, van Diest PJ, Hinrichs J, Bosch JL, Jans JJ (2010) Expression of nuclear FIH independently predicts overall survival of clear cell renal cell carcinoma patients. Eur J Cancer 46:3375–3382

Ku JH, Park YH, Myung JK, Moon KC, Kwak C, Kim HH (2011) Expression of hypoxia inducible factor-1α and 2α in conventional renal cell carcinoma with or without sarcomatoid differentiation. Urol Oncol 29:731–737

Laughner E, Taghavi P, Chiles K, Mahon PC, Semenza GL (2001) HER2 (neu) signaling increases the rate of hypoxia-inducible factor 1α (HIF-1α) synthesis: novel mechanism for HIF-1-mediated vascular endothelial growth factor expression. Mol Cell Biol 21:3995–4004

Lee S, Nakamura E, Yang H, Wei W, Linggi MS, Sajan MP, Farese RV, Freeman RS, Carter BD, Kaelin WG Jr, Schlisio S (2005) Neuronal apoptosis linked to EglN3 prolyl hydroxylase and familial pheochromocytoma genes: developmental culling and cancer. Cancer Cell 8:155–167

Lieb ME, Menzies K, Moschella MC, Ni R, Taubman MB (2002) Mammalian EGLN genes have distinct patterns of mRNA expression and regulation. Biochem Cell Biol 80:421–426

Lipscomb E, Sarmiere P, Crowder R, Freeman RS (1999) Expression of the SM-20 gene promotes death in nerve growth factor-dependent sympathetic neurons. J Neurochem 73:429–432

Lipscomb E, Sarmiere P, Freeman RS (2001) SM-20 is a novel mitochondrial protein that causes caspase-dependent cell death in nerve growth factor-dependent neurons. J Biol Chem 276:11775–11782

Marxsen JH, Stengel P, Doege K, Heikkinen P, Jokilehto T, Wagner T, Jelkmann W, Jaakkola P, Metzen E (2004) Hypoxia-inducible factor-1 (HIF-1) promotes its degradation by induction of HIF-α-prolyl-4-hydroxylases. Biochem J 381:761–767

Maxwell PH, Wiesener MS, Chang GW, Clifford SC, Vaux EC, Cockman ME, Wykoff CC, Pugh CW, Maher ER, Ratcliffe PJ (1999) The tumour suppressor protein VHL targets hypoxia-inducible factors for oxygen-dependent proteolysis. Nature 399:271–275

Maynard MA, Ohh M (2007) The role of hypoxia-inducible factors in cancer. Cell Mol Life Sci 64:2170–2180

Pescador N, Cuevas Y, Naranjo S, Alcaide M, Villar D (2005) Landázuri MO, del Peso L: identification of a functional hypoxia-responsive element that regulates the expression of the egl nine homologue 3 (egln3/phd3) gene. Biochem J 390:189–197

Pore N, Jiang Z, Shu HK, Bernhard E, Kao GD, Maity A (2006) Akt1 activation can augment hypoxia-inducible factor-1a expression by increasing protein translation through a mammalian target of rapamycin-independent pathway. Mol Cancer Res 4:471–479

Sato E, Torigoe T, Hirohashi Y, Kitamura H, Tanaka T, Honma I, Asanuma H, Harada K, Takasu H, Masumori N, Ito N, Hasegawa T, Tsukamoto T, Sato N (2008) Identification of an immunogenic CTL epitope of HIFPH3 for immunotherapy of renal cell carcinoma. Clin Cancer Res 14:6916–6923

Semenza GL, Wang GL (1992) A nuclear factor induced by hypoxia via de novo protein synthesis binds to the human erythropoietin gene enhancer at a site required for transcriptional activation. Mol Cell Biol 12:5447–5454

Shinojima T, Oya M, Takayanagi A, Mizuno R, Shimizu N, Murai M (2007) Renal cancer cells lacking hypoxia-inducible factor (HIF)-1α expression maintain vascular endothelial growth factor expression through HIF-2α. Carcinogenesis 28:529–536

Straub JA, Lipscomb EA, Yoshida ES, Freeman RS (2003) Induction of SM-20 in PC12 cells leads to increased cytochrome c levels, accumulation of cytochrome c in the cytosol, and caspase-dependent cell death. J Neurochem 85:318–328

Su Y, Loos M, Giese N, Hines OJ, Diebold I, Görlach A, Metzen E, Pastorekova S, Friess H, Büchler P (2010) PHD3 regulates differentiation, tumour growth and angiogenesis in pancreatic cancer. Br J Cancer 103:1571–1579

Tanaka T, Kitamura H, Torigoe T, Hirohashi Y, Sato E, Masumori N, Sato N, Tsukamoto T (2011) Autoantibody against hypoxia-inducible factor prolyl hydroxylase-3 is a potential serological marker for renal cell carcinoma. J Cancer Res Clin Oncol 137:789–794

Volpe A, Jewett MAS (2005) The natural history of small renal masses. Nat Clin Pract Urol 2:384–390

Wang GL, Semenza GL (1995) Purification and characterization of hypoxia-inducible factor 1. J Biol Chem 270:1230–1237

Wang GL, Jiang BH, Rue EA, Semenza GL (1995) Hypoxia-inducible factor 1 is a basic-helix-loop-helix-PAS heterodimer regulated by cellular O2 tension. Proc Natl Acad Sci USA 92:5510–5514

Yamamoto M, Torigoe T, Kamiguchi K, Hirohashi Y, Nakanishi K, Nabeta C, Asanuma H, Tsuruma T, Sato T, Hata F, Ohmura T, Yamaguchi K, Kurotaki T, Hirata K, Sato N (2005) A novel

isoform of TUCAN is overexpressed in human cancer tissues and suppresses both caspase-8- and caspase-9-mediated apoptosis. Cancer Res 65:8709–8714

Yu F, White SB, Zhao Q, Lee FS (2001) HIF-1α binding to VHL is regulated by stimulus-sensitive proline hydroxylation. Proc Natl Acad Sci USA 98:9630–9635

Zhong H, Agani F, Baccala AA, Laughner E, Rioseco-Camacho N, Isaacs WB, Simons JW, Semenza GL (1998) Increased expression of hypoxia inducible factor-1a in rat and human prostate cancer. Cancer Res 58:5280–5284

特集：Human Immunology：疾患理解から治療へ
総　説

がんワクチン創薬への道程
ーがん抗原の同定から臨床試験までー

鳥越俊彦，廣橋良彦，塚原智英，金関貴幸，Vitaly Kochin，佐藤昇志

The path to innovative drug development of cancer vaccine: From discovery of tumor antigens to clinical trials

Toshihiko Torigoe, Yoshihiko Hirohashi, Tomohide Tsukahara, Takayuki Kanaseki, Vitaly Kochin, and Noriyuki Sato

Department of Pathology 1, Sapporo Medical University School of Medicine

(Accepted February 17, 2014)

summary

Tumor immunology has been advancing after the great discovery of tumor-specific antigen MAGE in 1991, and a number of tumor antigens have been reported to date. We have also found novel tumor antigens through various methodologies such as gene expression cloning, bioinformatics, reverse immunology, transcriptome analysis and peptidome analysis. Recently, we made a success of defining cancer stem cell-specific antigens. The fruits of our basic research have been applied to clinical trials of cancer vaccine. The long path and future perspectives of innovative immunotherapeutic drug development are described.

Key words——tumor antigen; cancer stem cell; peptide vaccine; CTL; immunotherapy

抄　録

1991年のMAGE抗原の発見以来，腫瘍免疫学は急速に発展し，数多くのヒト腫瘍特異抗原が報告されている．著者らも，遺伝子発現クローニング法，バイオインフォマティクス，Reverse immunology，Transcriptome解析，網羅的ペプチド解析などの方法を駆使して，多くのヒト腫瘍抗原を同定してきた．近年，ヒト固形腫瘍の根幹をなすがん幹細胞の分離によって，がん幹細胞特異抗原も明らかにしてきた．一方で，これら基礎研究成果を創薬につなげるために，T細胞エピトープペプチドを用いたがんワクチン臨床試験も推進している．臨床試験ではワクチンの安全性，腫瘍抑制効果，免疫効果を検証し，最適プロトコルとバイオマーカーを見出さなければならない．臨床試験の結果を基礎研究にフィードバックし，より効果の高いがんワクチンの実用化をめざす創薬の道程と展望について概説する．

はじめに

著者らは過去30年以上にわたり，ヒトがん免疫について基礎研究および臨床研究を進めてきた．近年，大学発の研究成果を創薬につなげるトランスレーショナルリサーチが積極的に推進され，医師主導治験が実施できる環境が整ってきた．本レビューでは，これまでどのようながん抗原が同定され，どのように分類され，どのような臨床試験が行われているのか，基礎研究から臨床試験まで，これまでの道程を概説し今後の展望を述べる．

札幌医科大学医学部病理学第一講座

1．がん抗原遺伝子と抗原ペプチドの同定

(1) 自家腫瘍細胞・CTLクローンペアの樹立と遺伝子発現クローニング

著者らはまず，がん患者さんの腫瘍組織からがん細胞株を樹立し，同じ患者さんの末梢血リンパ球と混合培養することによって，自家腫瘍細胞と細胞障害性T細胞（CTL）クローンのペアを樹立した[1]．この腫瘍細胞に発現する遺伝子のライブラリーを293T細胞にトランスフェクションし，CTLクローンの活性化を指標とした発現クローニング法によって，HLA-B*5502拘束性に提示される腫瘍抗原遺伝子をスクリーニングした（**表1A**）[2]．

表1 札幌医科大学において同定された抗原分子とペプチド

がん種	抗原ペプチド（提示分子）	抗原タンパク質	文献
A） 自家腫瘍・CTL ペア			
胃がん	F4.2 (A31)	c98	32)
骨肉腫	PBF-B55 (B55)	PBF	2)
骨肉腫	PBF-A24 (A24)	PBF	33)
骨肉腫	PBF-A2 (A02)	PBF	34)
B） バイオインフォマティクス			
種々	HIFPH3-8 (A24)	HIFPH3	7)
種々	CEP55-193 (A24)	CEP55 (C10orf3)	3)
前立腺がん	AMACR2 (A24)	AMACR	6)
前立腺がん	STEAP-B (A24)	STEAP1	5)
肺がん	Lengsin-A02, A24 (A02, A24)	Lengsin	4)
C） Reverse Immunology			
1） アポトーシス関連			
種々	SVN-2B (A24)	Survivin 2B	11)
種々	C58 (A24)	Survivin	35)
種々	L7 (A24)	Livin	12)
2） 染色体転座			
滑膜肉腫	A (A24)	SYT-SSX1	9)
滑膜肉腫	B (A24)	SYT-SSX1	9)
滑膜肉腫	K9I (A24)	SYT-SSX1	10)
D） がん幹細胞			
種々	SOX2-109 (A24)	SOX2	36)
大腸がん	OR7C1-93 (A24)	OR7C1	
腎・大腸がん	DNAJB8-A24 (A24)	DNAJB8	25)
大腸がん	SF9 (A24)	FAM83B	

(2) 網羅的遺伝子発現解析と Reverse Immunology

2000 年代に DNA microarray 解析法や遺伝子発現データベースが発達したおかげで，網羅的な遺伝子発現解析が可能となった．著者らは正常組織と腫瘍組織にそれぞれ発現する遺伝子を比較し，正常組織には発現がほとんどなく，腫瘍組織に高発現する遺伝子群をスクリーニングすることによって，数種類の腫瘍抗原遺伝子を同定した（**表1 B**）[3-8]．

また滑膜肉腫には，遺伝子転座によって融合遺伝子産物 SYT-SSX1 が発現していることから，HLA 結合モチーフ検索によって HLA-A*2402 拘束性に提示される抗原ペプチドを同定した[9, 10]．同様に，腫瘍特異的に発現する Inhibitor of apoptosis protein family 分子 Survivin, Livin からも HLA-A*2402 拘束性抗原ペプチドを同定した（**表1 C**）[11, 12]．このように，既知のがん抗原から HLA 結合モチーフ検索によって抗原ペプチドをスクリーニングする方法は Reverse Immunology 法とよばれる[13, 14]．

(3) 網羅的 HLA 結合ペプチド解析

さらに近年著者らは，腫瘍細胞表面の HLA/ペプチド complex を免疫沈降し，マススペクトル解析によって HLA 結合ペプチドのアミノ酸配列を網羅的に分析する手法を確立した．ペプチドのアミノ酸配列情報から，親抗原タンパク質を推測することができる．推測された抗原遺伝子のなかから，腫瘍細胞に特異的発現を示す遺伝子を選別することによって，新たながん抗原遺伝子と抗原ペプチドを同定することに成功した（**表1** SF9/FAM83B）．Reverse Immuology 法によって同定される抗原ペプチドは，HLA 結合モチーフによって予測された仮想抗原ペプチド（Virtual Antigenic Peptide）であるのに対し，本方法によって同定されるペプチドは，実際に腫瘍細胞表面に提示されているナチュラル抗原ペプチド（Natural Antigenic Peptide, NAP）であることが特徴である．

2．がん抗原の種類とワクチン療法

(1) がん抗原の種類

このようにして多くのがん抗原遺伝子・ペプチドを同定してみると，がん抗原は大きく 3 種類に分類できることが判明した[15, 16]．1 つは SYT-SSX1 融合

遺伝子産物に代表されるような腫瘍細胞特異的な遺伝子変異・染色体転座に由来する抗原である．がん特異性という点では極めて理想的な抗原であるが，多くのヒト固形腫瘍では未知のままである．2つめは腫瘍細胞において過剰発現している抗原で，がん細胞の悪性形質と関連した機能をもつ分子が多く，アポトーシスを阻害するIAP family抗原や，シグナル伝達分子，細胞増殖・細胞周期関連分子が含まれる．これらの抗原は低レベルではあるが正常組織にも発現しており，免疫寛容のために抗原性が低いという欠点がある．3つめのグループは，Cancer-Testis (CT) antigensで，1991年にThierry Boonらによって発見されたMAGE-A1がその代表である[17]．正常組織では精巣にしか発現していない抗原で，現在までにCT1.1~CT136まで150種類以上のCT antigensが登録されている（GeneCards V3）．

近年著者らは，CT antigensの一部がヒト固形腫瘍のがん幹細胞に高発現しており，がん幹細胞標的抗原として免疫治療に有用であるばかりでなく，機能的にもがん幹細胞の造腫瘍性に重要な役割を果たしていることを見出している（**表1 D**）[18, 19]．著者らは，がん幹細胞特異的発現を示すCT antigensを，がん・精巣・幹細胞抗原（Cancer-Testis-Stem, CTS antigens）と呼び，現在がん幹細胞標的ワクチンを開発中である．

(2) がんワクチン療法の治療標的

がん幹細胞は，幹細胞様形質と高い造腫瘍能をもつ少数のがん細胞亜集団で，がんの治療抵抗性や再発・転移の主犯細胞であると考えられており，がん幹細胞を標的とした治療法の開発が現在世界中で進められている[16, 20]．がん抗原をがん幹細胞の観点から分類すると，がん幹細胞・非幹細胞共通抗原とそれぞれに特異的ながん抗原，正常幹細胞にも発現する抗原とに分類される（**図1**）[21, 22]．どのような抗原を標的としたワクチンが最も効果的であろうか？著者らは動物モデルを用いてがん予防モデル実験とがん治療モデル実験とを行った．その結果，いずれのモデルにおいてもがん幹細胞特異抗原を標的とする免疫治療でより高い腫瘍抑制効果が得られた（**図2**）[23]．抗がん剤に耐性をもつがん幹細胞も，細胞障害性T細胞（CTL）によって細胞障害を受けることが確認されており[21, 24, 25]，進行がんの治療および再発予防ワクチンとしての臨床効果が期待される．

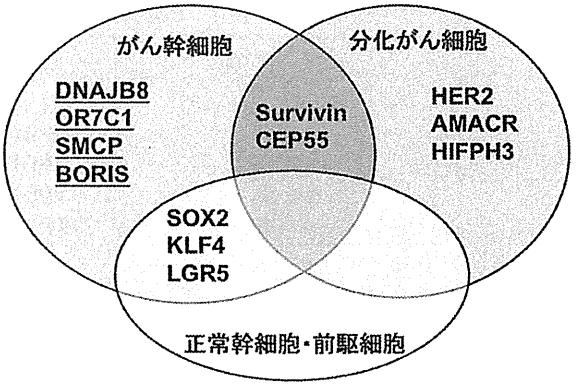

図1 がん幹細胞の観点から分類したがん抗原の種類
がん幹細胞，分化がん細胞および正常幹細胞における発現パターンから，がん抗原は大きく3種類に分類される．このうちアンダーラインをつけた抗原分子は，がん・精巣抗原である．

3．がんワクチン療法臨床試験

(1) 臨床試験の概要と結果

著者らは，これまでの基礎研究成果を創薬につなげるために，2004年からペプチドワクチンの臨床試験を開始した（**図3**）．Survivin由来のHLA-A*2402拘束性CTLエピトープSVN-2Bペプチドを2週間毎に4回皮下注射するワクチン試験では，RECIST判定によって腫瘍抑制効果を検証し，HLA/ペプチドテトラマー解析とELISPOT解析によって免疫効果を検証した[26]．免疫補助剤には，不完全フロイドアジュバンドとInterferon-α（IFN）を使用した[27-30]．

進行大腸がん（主に腺がん）と進行口腔がん（主に扁平上皮がん）のいずれを対象とした試験においても，IFNを併用した場合において，有意に高い腫瘍抑制効果と免疫効果（テトラマー解析）が得られることが判明した（**表2**）．IFN併用ワクチンを受けた術後再発進行膵臓がんの患者は8年間経過した現在も試験を継続中である．2012年より厚労省補助金を受けて医師主導治験を実施．「有効な治療法のない進行消化器がんを対象としたSVN-2B単独投与の第1相臨床試験」の結果，病勢コントロール率は53%（15例）で，そのうち進行膵臓がん10例を追跡調査した結果，全生存期間中央値は8.8ヵ月と延長が認められた．2013年より，「有効な治療法のない進行膵臓がんを対象としたプラセボ，SVN-2B単独投与，SVN-2B/IFN併用投与の二重盲検群間比較試験」を実施中である．

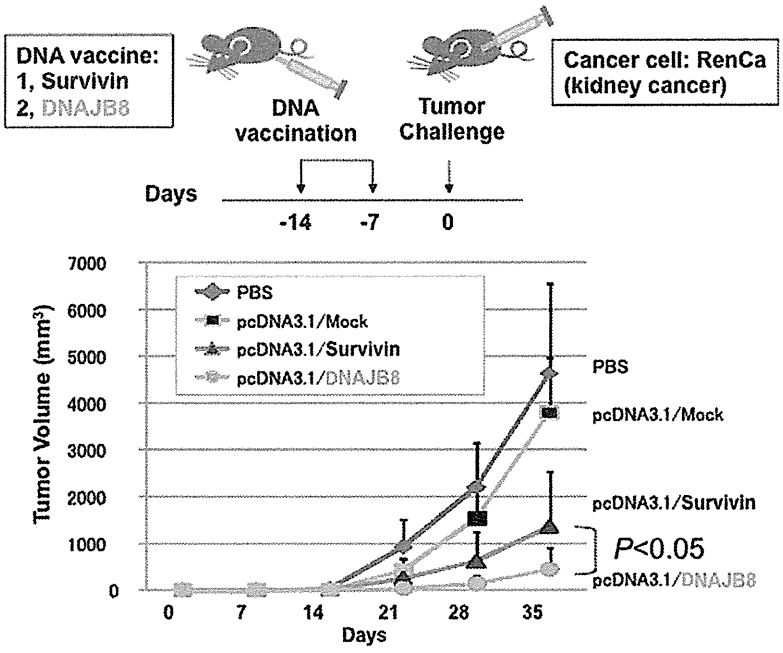

図2　がんワクチンのがん予防モデル実験
Survivin または DNAJB8 をコードする発現 Plasmid DNA を BALB/c マウスに 2 回免疫した後，同系腎がん細胞株 RenCa を移植した．がん幹細胞特異抗原 DNAJB8 を免疫した群で，有意に高い腫瘍抑制効果が認められた[18]．

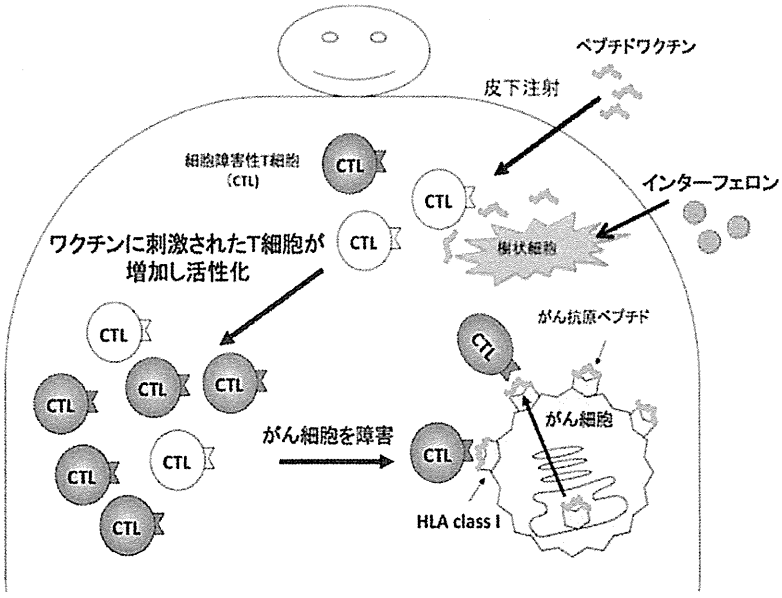

図3　がんワクチンの腫瘍抑制効果メカニズム
ペプチドワクチンを皮下注射すると，局所および所属リンパ節の樹状細胞の働きによってペプチド特異的 CTL が誘導され，体内で増殖する．CTL は抗原ペプチドを発現している腫瘍細胞を認識し，細胞障害活性を発揮する．インターフェロンは樹状細胞の活性化と腫瘍細胞の HLA class I 発現を促進する．

(2)　がんワクチン療法のバイオマーカー

CTL エピトープペプチドを用いたワクチンの特質の一つとして，ELISPOT 解析やテトラマー解析によってワクチン特異的 CTL 応答をモニタリングできるという特徴があげられる．実際に，SVN-2B ペプチドワクチン試験を受けた被験者のテトラマー解析結果と腫瘍抑制効果とを比較したところ，ワクチン投与前のテトラマー陽性 T 細胞が低い被験者に，比較的高い免疫効果と腫瘍抑制効果が認められることが判明した．

表 2　SVN-2B 臨床試験の結果（自主臨床研究）

がん種とプロトコール	副作用	評価症例数	腫瘍抑制効果 (PR, SD割合)	テトラマー解析 特異的CTL増加%
大腸がん				
SVN-2Bのみ	無	15	27% (4/15)	13% (2/15)
SVN-2B + IFA	無	5	20% (1/5)	0% (0/5)
SVN-2B + IFA + IFNα	発熱	8	50% (4/8)	75% (6/8)
IFNαのみ	発熱	3	0% (0/3)	0% (0/3)
膵臓がん				
SVN-2B + IFA + IFNα	発熱	6	66% (4/6)	66% (4/6)
口腔がん				
SVN-2B のみ	無	8	12% (1/8)	75% (6/8)
SVN-2B + IFA + IFNα	発熱	6	50% (3/6)	100% (6/6)
膀胱がん				
SVN-2B + IFA	発熱	9	22% (2/9)	56% (5/9)

腫瘍抑制効果は CT 画像を RECIST に基づいて評価した．テトラマー解析は，ワクチン前と比較してワクチン後のテトラマー陽性 CTL 数が 1.5 倍以上増加した症例を CTL 増加症例とした．IFA: 不完全フロイドアジュバンド．
IFNα: Interferon-α

また，ホルマリン固定組織標本の HLA class I 発現を免疫染色によって検出できる単クローン抗体 EMR8-5 を樹立し[31]，原発腫瘍組織の発現レベルと腫瘍抑制効果とを比較したところ，HLA class I 陰性と判定された被験者は，癌種にかかわらず全例で腫瘍抑制効果が認められなかった[14]．がんワクチン療法の効果予測マーカーとして，テトラマー解析法と HLA class I 免疫組織染色法は極めて有用であると考えられた．

4．今後の展望

臨床試験の先行しているがん抗原 Survivin はがん幹細胞・非幹細胞共通抗原であり，一方でがん幹細胞特異抗原（CTS antigens）の 1 つ OR7C1 を標的とするワクチンの臨床試験を現在準備中である．ヒトの臨床試験においても動物モデル試験と同様の結果が認められるのかどうか，大変興味深い．CTL エピトープだけでなく，ヘルパーペプチドの有用性を検証する臨床試験も重要である．また，不完全フロイドアジュバンドや IFN よりも有効性の高い免疫補助剤を開発することも今後の重要な課題である．

第 1 世代がんワクチンの安全性と有効性を治験によって正確かつ客観的に実証することが求められているが，どのような抗原を標的として，何をモニタリングしながら，どのような投与方法・投与間隔で，どのような構造のペプチドを投与すれば良いのか，課題が多く残されている．臨床試験の結果を基礎研究にフィードバックしながら，次世代がんワクチンの開発を急ぎたい．

文　献

1) Nabeta, Y., et al.: Recognition by cellular and humoral autologous immunity in a human osteosarcoma cell line. *J Orthop Sci.* **8**: 554–559, 2003.
2) Tsukahara, T., et al.: Identification of human autologous cytotoxic T-lymphocyte-defined osteosarcoma gene that encodes a transcriptional regulator, papillomavirus binding factor. *Cancer Res.* **64**: 5442–5448, 2004.
3) Inoda, S., et al.: Cep55/c10orf3, a tumor antigen derived from a centrosome residing protein in breast carcinoma. *J Immunother.* **32**: 474–485, 2009.
4) Nakatsugawa, M., et al.: Novel spliced form of a lens protein as a novel lung cancer antigen, Lengsin splicing variant 4. *Cancer Sci.* **100**: 1485–1493, 2009.
5) Yamamoto, T., et al.: Six-transmembrane epithelial antigen of the prostate-1 plays a role for in vivo tumor growth via intercellular communication. *Experimental cell research.* **17**: 2617–2626, 2013.
6) Honma, I., et al.: Aberrant expression and potency as a cancer immunotherapy target of alpha-methylacyl-coenzyme A racemase in prostate cancer. *J Transl Med.* **7**: 103, 2009.
7) Sato, E., et al.: Identification of an immunogenic CTL epitope of HIFPH3 for immunotherapy of renal cell carcinoma. *Clin Cancer Res.* **14**: 6916–6923, 2008.
8) Nakatsugawa, M., et al.: Identification of an HLA-A*0201-restricted cytotoxic T lymphocyte epitope from the lung carcinoma antigen, Lengsin. *Int J Oncol.* **39**: 1041–1049, 2011.
9) Sato, Y., et al.: Detection and induction of CTLs specific for SYT-SSX-derived peptides in HLA-A24(+) patients with synovial sarcoma. *J Immunol.* **169**: 1611–1618, 2002.
10) Ida, K., et al.: Crisscross CTL induction by SYT-SSX junction peptide and its HLA-A*2402 anchor substitute. *J Immunol.* **173**: 1436–1443, 2004.
11) Hirohashi, Y., et al.: An HLA-A24-restricted Cytotoxic T Lymphocyte Epitope of a Tumor-associated Protein, Survivin. *Clin Cancer Res.* **8**: 1731–1739, 2002.
12) Hariu, H., et al.: Aberrant expression and potency as a cancer immunotherapy target of inhibitor of apoptosis protein family, Livin/ML-IAP in lung cancer. *Clin Cancer Res.* **11**: 1000–1009, 2005.
13) Hirohashi, Y., et al.: The functioning antigens: beyond just as the immunological targets. *Cancer*

Sci. **100**: 798–806, 2009.

14) Sato, N., et al.: Molecular pathological approaches to human tumor immunology. *Pathol Int.* **59**: 205–217, 2009.

15) Hirohashi, Y., et al.: Cytotoxic T lymphocytes: Sniping cancer stem cells. *Oncoimmunology.* **1**: 123–125, 2012.

16) Hirohashi, Y., et al.: Immune response against tumor antigens expressed on human cancer stem-like cells/tumor-initiating cells. *Immunotherapy.* **2**: 201–211, 2010.

17) van der Bruggen, P., et al.: A gene encoding an antigen recognized by cytolytic T lymphocytes on a human melanoma. *Science* (New York, NY). **254**: 1643–1647, 1991.

18) Nishizawa, S., et al.: HSP DNAJB8 controls tumor-initiating ability in renal cancer stem-like cells. *Cancer Res.* **72**: 2844–2854, 2012.

19) Yamada, R., et al.: Preferential expression of cancer/testis genes in cancer stem-like cells: proposal of a novel sub-category, cancer/testis/stem gene. *Tissue antigens.* **81**: 428–434, 2013.

20) Saijo, H., et al.: Cytotoxic T lymphocytes: the future of cancer stem cell eradication? *Immunotherapy.* **5**: 549–551, 2013.

21) Inoda, S., et al.: Cytotoxic T lymphocytes efficiently recognize human colon cancer stem-like cells. *The American journal of pathology.* **178**: 1805–1813, 2011.

22) Mori, T., et al.: Efficiency of G2/M-related tumor-associated antigen-targeting cancer immunotherapy depends on antigen expression in the cancer stem-like population. *Exp Mol Pathol.* **92**: 27–32, 2012.

23) Nishizawa, S., et al.: Heat shock protein DNAJB8 controls tumor-initiating ability in renal cancer stem-like cells. *Cancer Res*, 2012.

24) Kano, M., et al.: Autologous CTL response against cancer stem-like cells/cancer-initiating cells of bone malignant fibrous histiocytoma. *Cancer Sci.* **102**: 1443–1447, 2011.

25) Morita, R., et al.: Heat shock protein DNAJB8 is a novel target for immunotherapy of colon cancer-initiating cells. *Cancer Sci*, 2014 (in press).

26) Tsuruma, T., et al.: Clinical and immunological evaluation of anti-apoptosis protein, survivin-derived peptide vaccine in phase I clinical study for patients with advanced or recurrent breast cancer. *J Transl Med.* **6**: 24, 2008.

27) Honma, I., et al.: Phase I clinical study of anti-apoptosis protein survivin-derived peptide vaccination for patients with advanced or recurrent urothelial cancer. *Cancer Immunol Immunother.* **58**: 1801–1807, 2009.

28) Miyazaki, A., et al.: Phase I clinical trial of survivin-derived peptide vaccine therapy for patients with advanced or recurrent oral cancer. *Cancer Sci.* **102**: 324–329, 2011.

29) Kameshima, H., et al.: Immunogenic enhancement and clinical effect by type-I interferon of anti-apoptotic protein, survivin-derived peptide vaccine, in advanced colorectal cancer patients. *Cancer Sci.* **102**: 1181–1187, 2011.

30) Kameshima, H., et al.: Immunotherapeutic benefit of alpha-interferon (IFNalpha) in survivin2B-derived peptide vaccination for advanced pancreatic cancer patients. *Cancer Sci.* **104**: 124–129, 2013.

31) Torigoe, T., et al.: Establishment of a monoclonal anti-pan HLA class I antibody suitable for immunostaining of formalin-fixed tissue: Unusually high frequency of down-regulation in breast cancer tissues. *Pathol Int.* **62**: 303–308, 2012.

32) Sahara, H., et al.: A Gene Encoding Human Gastric Signet Ring Cell Carcinoma Antigen Recognized by HLA-A31-Restricted Cytotoxic T Lymphocytes. *J Immunother.* **25**: 235–242, 2002.

33) Tsukahara, T., et al.: Prognostic impact and immunogenicity of a novel osteosarcoma antigen, papillomavirus binding factor, in patients with osteosarcoma. *Cancer Sci.* **99**: 368–375, 2008.

34) Tsukahara, T., et al.: HLA-A*0201-restricted CTL epitope of a novel osteosarcoma antigen, papillomavirus binding factor. *J Transl Med.* **7**: 44, 2009.

35) Kobayashi, J., et al.: Comparative study on the immunogenicity between an HLA-A24-restricted cytotoxic T-cell epitope derived from survivin and that from its splice variant survivin-2B in oral cancer patients. *J Transl Med.* **7**: 1, 2009.

36) Nakatsugawa M, et al.: SOX2 is overexpressed in stem-like cells of human lung adenocarcinoma and augments the tumorigenicity. *Laboratory investigation.* **91**: 1796–1804, 2011.

THE JOURNAL OF BIOLOGICAL CHEMISTRY VOL. 289, NO. 32, pp. 22035–22047, August 8, 2014

Specific Targeting of a Naturally Presented Osteosarcoma Antigen, Papillomavirus Binding Factor Peptide, Using an Artificial Monoclonal Antibody*[S]

Received for publication, March 30, 2014, and in revised form, June 9, 2014 Published, JBC Papers in Press, June 24, 2014, DOI 10.1074/jbc.M114.568725

Tomohide Tsukahara[‡1], Makoto Emori[§], Kenji Murata[‡§], Takahisa Hirano[¶], Norihiro Muroi[¶], Masanori Kyono[¶], Shingo Toji[‖], Kazue Watanabe[‖], Toshihiko Torigoe[‡], Vitaly Kochin[‡], Hiroko Asanuma[**], Hiroshi Matsumiya[‡‡], Keiji Yamashita[‡‡], Tetsuo Himi[‡‡], Shingo Ichimiya[§§], Takuro Wada[§], Toshihiko Yamashita[§], Tadashi Hasegawa[**], and Noriyuki Sato[‡]

From the [‡]Department of Pathology, [¶]M.D./Ph.D. program, and [§§]Department of Immunology, Frontier Medical Research Center, Sapporo Medical University School of Medicine, Sapporo 060-8556, Japan, [§]Department of Orthopaedic Surgery, Sapporo Medial University School of Medicine, Sapporo 060-8543, Japan, [‖]Ina Laboratory, Medical and Biological Laboratories Company, Limited, Ina 396-0002, Japan, [**]Division of Surgical Pathology, Sapporo Medical University Hospital, Sapporo 060-8543, Japan, [‡‡]Department of Otolaryngology, Sapporo Medical University School of Medicine, Sapporo 060-8543, Japan

Background: Peptide vaccine-based immunotherapy targeting tumor-associated antigens can elicit CTL responses. However, the expression status of HLA·vaccinated peptide complexes on tumor cells is unknown.
Results: Using a phage display, we isolated mAb D12, which reacted with an HLA-A2·PBF peptide.
Conclusion: We successfully detected the HLA·peptide complex on osteosarcoma cells.
Significance: Assessment of HLA·peptide complexes is important to predict the effect of immunotherapy.

Osteosarcoma is a rare but highly malignant tumor occurring most frequently in adolescents. The prognosis of non-responders to chemotherapy is still poor, and new treatment modalities are needed. To develop peptide-based immunotherapy, we previously identified autologous cytotoxic T lymphocyte-defined osteosarcoma antigen papillomavirus binding factor (PBF) in the context of HLA-B55 and the cytotoxic T lymphocyte epitope (PBF A2.2) presented by HLA-A2. PBF and HLA class I are expressed in ~90 and 70% of various sarcomas, respectively. However, the expression status of peptide PBF A2.2 presented by HLA-A2 on osteosarcoma cells has remained unknown because it is difficult to generate a specific probe that reacts with the HLA·peptide complex. For detection and qualification of the HLA-A*02:01·PBF A2.2 peptide complex on osteosarcoma cells, we tried to isolate a single chain variable fragment (scFv) antibody directed to the HLA-*A0201·PBF A2.2 complex using a naïve scFv phage display library. As a result, scFv clone D12 with high affinity ($K_D = 1.53 \times 10^{-9}$ M) was isolated. D12 could react with PBF A2.2 peptide-pulsed T2 cells and HLA-A2+PBF+ osteosarcoma cell lines and simultaneously demonstrated that the HLA·peptide complex was expressed on osteosarcoma cells. In conclusion, scFv clone D12 might be useful to select candidate patients for PBF A2.2 peptide-based immunotherapy and develop antibody-based immunotherapy.

Osteosarcoma is the most common primary malignant tumor of bone. The survival rate of patients with this disease was under 20% before 1970. Since then, the introduction of neoadjuvant chemotherapy, establishment of guidelines for adequate surgical margins, and development of postexcision reconstruction have raised the 5-year survival rate to 60–70% (1, 2). These advances overshadowed the pioneering adjuvant immunotherapy trials using autologous tumor vaccines for patients with osteosarcoma despite their having some therapeutic efficacy (3–5). However, the survival rate of patients with osteosarcoma has reached a plateau in the last decade (6), which has reignited interest in immunotherapeutic approaches (7–10).

Peptide vaccine-based immunotherapy targeting tumor-associated antigens could elicit CTL[2] responses against HLA·peptide complexes. Therefore, expression of targeted HLA·peptide complexes on tumor cells is prerequisite for peptide vaccination. However, the detection and visualization of HLA·peptide complexes is very difficult because (i) it is still hard to establish CTL clones directed to HLA·peptide complexes, (ii) the affinity of soluble natural TCR obtained from CTL clones is not sufficient to visualize HLA·peptide complexes, (iii) generation of anti-HLA·peptide monoclonal antibodies using immunized mice is very difficult, and (iv) the

* This work was supported by grants from Japan Society for the Promotion of Science Grants-in-aid for Scientific Research (KAKENHI) 21249025 (to N. S.), 20390403 (to T. W.), and 22689041 and 25462344 (to T. Tsukahara); Management Expenses Grants 23-A-10 (to T. W.) and 23-A-44 (to N. S.) from the Government to the National Cancer Center; and Northern Advancement Center for Science and Technology Grant H24-S-5, Takeda Science Foundation Grant 2010-Kenkyu-Shorei, and Suhara Memorial Foundation Grant H24-12 (to T. Tsukahara).
[S] This article contains supplemental Table S1.
[1] To whom correspondence should be addressed: Dept. of Pathology, Sapporo Medical University School of Medicine, West 17, South 1, Chuo-ku, Sapporo 060-8556, Japan. Tel.: 81-11-611-2111; Fax: 81-11-643-2310; E-mail: tukahara@sapmed.ac.jp.

[2] The abbreviations used are: CTL, cytotoxic T lymphocyte; PBF, papillomavirus binding factor; scFv, single chain variable fragment; OS, osteosarcoma; MFH, malignant fibrous histiocytoma; VH, variable regions of heavy chains; VL, variable regions of light chains; Vκ, variable regions of VLκ chains and Vl, variable regions of VLλ chains; YT, yeast extract-tryptone; hIgG, human IgG; MFI, mean fluorescence intensity; TCR, T cell receptor.

amount of a specific HLA·peptide complex on cells might be too low to detect. Therefore, although generation of anti-HLA·vaccine peptide complex antibodies is very attractive, it remains challenging.

Papillomavirus binding factor (PBF) was first identified as a transcription factor regulating promotor activity on the human papillomavirus type 8 genome (11). We demonstrated that PBF was an osteosarcoma-associated antigen recognized by an autologous cytotoxic T lymphocyte clone (12). Immunohistochemical analysis revealed that 92% of biopsy specimens of osteosarcoma expressed PBF. Moreover, PBF-positive osteosarcoma has a significantly poorer prognosis than that with negative expression of PBF (13). Generally, conventional osteosarcoma is a malignant neoplasm of mesenchymal origin, and there is no specific cause such as viral infection (14). It is suggested that PBF has certain functions not only in transcription of the human papillomavirus genome but also in the cell survival and apoptosis of osteosarcoma (15, 16), innate immunity (17), and adipogenesis (18). Conversely, HLA class I is also expressed in 68% of primary osteosarcoma tissues and correlated with good prognosis (19). These findings suggest that osteosarcoma might be immunogenic for cellular immunity. Next, we identified the CTL epitopes in the context of HLA-A24 and HLA-A2 by a reverse immunology approach (13, 20). We are currently conducting a clinical phase I trial of peptide vaccination therapy for patients with osteosarcoma using these epitopes. Obviously, the expression status of PBF and HLA class I can be assessed by standard immunohistochemistry. However, the expression status of the HLA class I·CTL epitope complex on osteosarcoma cells is still unknown because of the difficulty of visualization of HLA·peptide complexes.

In this study, with the aim to characterize of the expression status of various HLA·peptide complexes on tumor cells, we constructed a naïve single chain variable fragment (scFv) phage display library and generated an artificial scFv antibody that reacts with an HLA·peptide complex using the PBF-derived peptide (PBF A2.2) in the context of HLA-A2 as a prototype antigen. Subsequently, we tried to detect the HLA-A2·PBF A2.2 peptide complex on osteosarcoma cells.

EXPERIMENTAL PROCEDURES

The present study was approved by the Ethics Committee of Sapporo Medical University. The patients, their families, and healthy donors provided informed consent for the use of blood samples and tissue specimens in our research.

Cell Lines

Five human osteosarcoma (OS) cell lines (U2OS, OS2000, KIKU, Saos-2, and HOS) and one bone human malignant fibrous histiocytoma (MFH) cell line (MFH2003) were used. The transporter associated with antigen processing (TAP)-deficient cell line T2 was also used. OS2000, KIKU, and MFH2003 were established in our laboratory (21–23). The other cell lines were kindly donated or purchased from the Japanese Collection of Research Bioresources Cell Bank (Tokyo, Japan) and American Type Culture Collection (Manassas, VA). MFH2003 and OS2000 were cultured with Iscove's modified Dulbecco's Eagle's medium (Invitrogen) containing 10% FBS, and the others were maintained in Dulbecco's modified Eagle's medium (DMEM; Sigma-Aldrich) containing 10% FBS in a 5% CO_2 incubator at 37 °C.

One primary culture of OS cells was used. Fresh specimens taken at surgery from the primary tumor in the left distal femur of a 15-year-old female were minced into small pieces and separately cultured with Iscove's modified Dulbecco's Eagle's medium containing 10% FBS in a 5% CO_2 incubator. When the cells grew to confluence, half were trypsinized and passaged. After 30 passages, cultured cells were used for the study. Malignant features of cultured cells were confirmed by cytodiagnosis.

Biotinylated Antigens and Peptides

Biotinylated HLA-A*02:01·peptide complex monomers were constructed by Medical and Biological Laboratories, Co., Ltd. (Nagoya, Japan). Peptides PBF A2.2 (ALPSFQIPV), HIV-A2 (SLYNTVATL), CMV-A2 (NLVPMVATV), Epstein-Barr virus LMP1 (YLQQNWWTL), NY-ESO-1 (SLLMWITQC), WT1 (RMFPNAPYL), human T-lymphotropic virus type I Tax1 (LLFGYPVYV), human T-lymphotropic virus type I Tax2 (QLGAFLTNV), MPT51 (TALGKGISVV), MART-1 (ELAGIGILTV), influenza M1 (GILGFVFTL), gp100M (IMDQVPFSV), tyrosinase (YMDGTMAQV), and gp100 (KTWGQYWQV) were used in the present study.

Construction of scFv Library from Naïve Donors

Construction of the Phagemid Vector pMARXL—We first constructed a phagemid vector based on pMod1 (a kind gift from Dr. Potjamas Pansti, Aarhus University, Aarhus, Denmark) (24). A point mutation at the XhoI site of the ampicillin resistance gene and linker peptide between the cloning sites of variable regions of heavy and light chains (VH and VL, respectively) were introduced into pMod1 as follows. The point mutation was introduced into the XhoI site of the ampicillin resistance gene of pMod1 with a PrimeSTAR Mutagenesis Basal kit using primers AmpR XhoI-mutation sense (5′-TGGGTGCACGAGTGGGTTACATCGAAC-3′) and AmpR XhoI-mutation antisense (5′-CCACTCGTGCACCCAACTGATCTTCAG-3′) according to the manufacturer's protocol. The resultant mutant was digested with XhoI and NotI followed by electrophoresis, cutting, and gel extraction using a QIAEX II Gel Extraction kit (Qiagen, Hilden, Germany). Next, two oligonucleotides containing XhoI-peptide linker-NheI-NotI (sense, 5′-TCGAGGGTGGAGGCGGTTCAGGCGGAGGTGGCTCTGGCGGTGGCGCTAGCGGCAGATCTGATGACGC-3′; antisense, 5′-GGCCGCGTCATCAGATCTGCCGCTAGCGCCACCGCCAGAGCCACCTCCGCCTGAACCGCCTCCACCC-3′) were denatured, annealed, and ligated into the digested vector using DNA Ligation kit version 2 (Takara) followed by transformation of *Escherichia coli* DH5α. The resultant vector was designated pMARXL (see Fig. 1).

scFv phage display libraries were constructed according to the methods described by Pansri *et al.* (24) and Schofield *et al.* (25) with some modifications to optimize the experimental conditions. The primers used for the amplification of variable regions are listed in supplemental Table S1.

Source and cDNA Preparation—Peripheral blood mononuclear cells of 31 healthy volunteers and two surgically resected

tonsils were used as RNA sources. Peripheral blood mononuclear cells were separately isolated from 50 ml of peripheral blood from each donor followed by total RNA extraction using an RNeasy Mini kit (Qiagen). Total RNA of the tonsils was separately extracted using an RNeasy Maxi kit (Qiagen). mRNA was isolated from each RNA using an Oligotex-dT30 <Super> mRNA Purification kit (Takara, Otsu, Japan). Thirty-one mRNA samples were divided and gathered into six groups (five to six mRNA samples per group). mRNAs of the two tonsils were gathered into a separate group. Then the mRNAs of the seven groups were converted into cDNAs with a First-Strand cDNA Synthesis kit (GE Healthcare). For reverse transcription, the specific primers for the κ and λ light chains and IgM heavy chain were used.

Primary PCR—Amplification of VH and VL was performed with DNA polymerase KODplus (Toyobo) using cDNA and the primers to amplify variable regions of VH and VL including the κ and λ chains (Vk and Vl, respectively). All 5′ primers (14 VH primers, 13 Vk primers, and 15 Vl primers) were used separately for PCR. 3′ primers for VH (four primers), Vk (five primers), and VL (three primers) were mixed in each group and used. Therefore, 294 PCRs were performed separately. The PCR mixture was denatured at 94 °C for 2 min followed by 35 cycles at 94 °C for 15 s, 55 °C for 30 s, and 68 °C for 1 min. Amplicons of VH, Vk, and Vl were electrophoresed (see Fig. 2*A*). The bands around 350 bp containing VH, Vk, and Vl were cut out, and cDNAs were separately extracted.

Secondary PCR—Extracted cDNA was used for secondary PCR to introduce restriction enzyme sites. PCR was performed using 1/10 of each amplicon as the template and primers. 5′ primers of 14 VH with mixed 3′-primers (four primers), 5′ primers of three Vk with mixed 3′ primers (five primers), and 5′ primers of three Vl with mixed 3′ primers (three primers) were used. The PCR mixture was denatured at 94 °C for 2 min followed by 35 cycles at 94 °C for 15 s, 55 °C for 30 s, and 68 °C for 1 min. Restriction site-introduced amplicons of 14 VH, three Vk, and three Vl were confirmed by electrophoresis (see Fig. 2*B*). These amplicons were gathered into 17 groups (VH1, VH2, VH3, VH4, VH5, VH6, VH7, Vk1, Vk2, Vk3, Vk4, Vk5, Vk6, Vl1–2, Vl3, Vl4–6, and Vl7–10) and purified with a column (QIAquick PCR Purification kit, Qiagen).

Construction of Initial Library of VH, Vk, and Vl—Purified cDNA of VH was digested with SfiI at 50 °C for 2 h followed by purification with the column and digestion with XhoI at 37 °C for 2 h. cDNAs of Vk and Vl were digested with NheI at 37 °C for 2 h followed by purification using the column and digestion with NotI at 37 °C for 2 h. The digested cDNA was electrophoresed, cut, and extracted as with primary PCR products. cDNA of VH was ligated into dephosphorylated pMARXL digested with SfiI and XhoI using a Rapid DNA Dephos and Ligation kit (Roche Diagnostics GmbH). All large scale ligation reactions were performed at 16 °C overnight. cDNAs of Vk and Vl were subcloned into pMARXL digested with NheI and NotI. Ligation products were purified with a column and electroporated into DH12S (Invitrogen). These were the initial libraries of VH and VL (Table 1).

Construction of the scFv Library—Inserts of VH were prepared from the initial libraries and digested with SfiI and XhoI followed by electrophoresis, cutting, and gel extraction. Vector DNAs coding Vk and Vl were prepared from the initial libraries and digested with SfiI and XhoI followed by dephosphorylation. All κ and λ libraries were combined into one group. Insert cDNAs and vector DNAs were ligated, purified, and electroporated into competent TG1 cells (Lucigen Corp., Middleton, WI). Transformed *E. coli* were plated on a 1.5% agarose gel of 2× YT containing ampicillin (100 μg/ml) and 2% glucose (2× YTAG) followed by the collection of all colonies into 2× YT liquid. Aliquots of *E. coli* were divided and frozen with 20% glycerol. In addition, scFv libraries of VH3-Vk1 and VH3-Vl6 were also prepared. These were the main scFv libraries (Table 1).

Construction of Additional scFv Libraries—To construct additional libraries of VH3-VK1 and VH3-Vl6, the primary PCR products of heavy chains (VH3a, VH3b, and VH3c) and light chains (Vk1a, Vk1b, Vk1c, Vk1d, and Vl6) were used independently for secondary PCR to introduce restriction enzyme sites and linker sequences with the primers listed in supplemental Table S1 followed by column purification, electrophoresis, cutting, and gel extraction. cDNAs of VH3 and VL (Vk1 and Vl6, respectively) were assembled by PCR. Equal amounts of cDNAs of heavy and light chains were used in the reaction mixture without primers. The PCR mixture was denatured at 94 °C for 2 min followed by five cycles at 94 °C for 30 s and 68 °C for 1 min. The reaction products were used for pull-through PCR containing the primers PT-BAKSfi (5′-GTCCTCGCAACTGCGGCCCAGCCGGCCATGGCC-3′) and PT-FORNot (5′-GAGTCATTCTCGACTTGCGGCCGCAC-3′). The mixture was denatured at 94 °C for 2 min followed by 30 cycles at 94 °C for 15 s, 55 °C for 30 s, and 68 °C for 1 min followed by column purification. Assembled cDNAs of VH and VL were digested with SfiI followed by digestion with NotI. After column purification, digested cDNA was ligated into digested and dephosphorylated pMARXL. After column purification, phagemids were electroporated into competent TG1. Transformed *E. coli* were plated on 2× YTAG plates followed by the collection of all colonies into 2× YT liquid. Aliquots of *E. coli* were divided and frozen. The additional libraries were VH3-Vk1 and VH3-Vl6 (Table 1).

Titration—E. coli electroporated with the library phagemid or infected with phages were serially diluted and plated on 2× YTAG plates followed by incubation at 37 °C overnight. The next day, the number of independent colonies was counted, and the titer was calculated.

Preparation of Primary Stocks and Rescue of the Libraries—Glycerol stock of each library was added to 500 ml of 2× YTAG liquid and incubated at 37 °C for 2 h. Cultured liquid containing *E. coli* was divided into aliquots of 1 ml/tube and cryopreserved with glycerol at −80 °C. These were the primary stocks of the libraries. These primary stocks were rescued as follows. Glycerol stocks of all the libraries were added to 25 ml of 2× YTAG liquid and shaken at 37 °C for 60–90 min until the A_{600} reached 0.5–1.0 followed by addition of 2.5×10^{10} of M13K07 (Invitrogen). After a 60-min incubation, *E. coli* were centrifuged. The pellet of *E. coli* was resuspended in fresh 2× YT containing ampicillin and kanamycin (25 μg/ml) and incubated with shaking at 30 °C overnight.

PEG Precipitation—The overnight culture of *E. coli* was centrifuged at 1000 × *g* for 20 min at 4 °C. The supernatant containing phage particles was collected, and ⅕ volume of 20% polyethylene glycol with 2.5 M NaCl was added followed by incubation on ice for more than 1 h. The phage was pelleted by centrifugation at 12,000 × *g* for 10 min at 4 °C, and then it was suspended with 4 ml of PBS, filtrated with a 0.45-μm filter, and used for biopanning.

Biopanning with Biotinylated Antigen

Before biopanning, the phage library (0.25 ml) was mixed with PBS containing 4% (w/v) milk (4% PBS-M) in a 1.5-ml tube and incubated with 100 μl of magnetic beads (Dynabeads M-280 Streptavidin, Invitrogen) that were prewashed with PBS with 0.1% Tween 20 (PBS-T) at room temperature for 60 min. After incubation, the phage supernatant was harvested on a magnetic stand. This step can remove nonspecific phages.

Biopanning was performed as follows. 100 μl of the magnetic beads was prewashed with PBS-T and blocked with 2% PBS-M for 1–2 h at room temperature. The phage supernatant was mixed with 0.5 ml of biotinylated antigen (500 nM in the first round and 100 nM in PBS in the second and subsequent ones) and mixed at room temperature for 60 min. After incubation, the phage-antigen mixture was mixed with the magnetic beads followed by additional incubation for 15 min. Then the beads were washed six times with 1 ml of 2% PBS-M with 0.1% Tween 20 and twice with 1 ml of PBS. Specific phage binders were eluted from the magnetic beads by incubation with 1 ml of 100 mM triethylamine for 7 min. The eluted phage aliquot was immediately neutralized with 100 μl of 1 M Tris-HCl (pH 7.4). Next, the resultant phage aliquot was used for phage rescue.

Phage rescue was performed as follows. Half of the phage aliquot after biopanning was added to 10 ml of log-phase TG1 and incubated at 37 °C for 1 h with slow shaking. This step allowed the phage to infect TG1. After incubation, ampicillin (final concentration, 100 μg/ml), glucose (final concentration, 20% (w/v)), and more than 1×10^{10} pfu of helper phage M13K07 was added and incubated for 60 min. Cultured TG1 infected with the phage and M13K07 was centrifuged at 2500 × *g* for 5 min and resuspended with 25 ml of fresh 2× YT containing ampicillin (100 μg/ml) and kanamycin (25 μg/ml) without glucose followed by incubation in a new flask at 30 °C overnight. The overnight culture of bacteria including the proliferated phage was isolated by PEG precipitation and used for the next round of biopanning.

Preparation of Log-phase TG1

TG1 was plated on agar plates of M9 minimal medium with 1 mM thiamine hydrochloride and 0.1% glucose. After overnight incubation at 37 °C, a single colony was inoculated into 100 ml of 2× YT medium followed by overnight incubation at 37 °C. A 1-ml aliquot of *E. coli* was inoculated into 100 ml of 2× YT and incubated at 37 °C with fast shaking for 90–120 min until the A_{600} value reached 0.5–1.0. The resultant *E. coli* were used as the log-phase TG1 for phage rescue.

Screening Specific Phage Clones Binding to the Biotinylated Antigen

After biopanning, soluble scFv expression of TG1 infected with the phage was induced in a microplate. Half of the phage aliquot after biopanning was added to 10 ml of log-phase TG1 and incubated at 37 °C for 1 h with slow shaking. After incubation, the aliquot of *E. coli* was diluted, seeded on a 2× YTAG plate, and incubated at 30 °C overnight. The next day, 94 clones were picked up and inoculated independently into wells containing 150 μl of 2× YTAG in a 96-well microculture plate. The plate was incubated at 30 °C with shaking overnight for phage rescue. The following day, 10 μl of cultured *E. coli* in each well was inoculated into 100 μl of 2× YTAG in a new 96-well microculture plate. The plate was incubated at 30 °C for 5–6 h. After incubation, the plate was centrifuged at 1000 × *g* for 5 min followed by replacement of the medium with 100 μl of 2× YT containing ampicillin and 1 mM isopropyl 1-thio-β-D-galactopyranoside. Then the plate was incubated at 30 °C overnight. After incubation, it was centrifuged at 1000 × *g* for 10 min. Then 50 μl of the supernatant was harvested and immediately used for ELISA screening.

For ELISA, 100 μl of biotinylated antigen (5 μg/ml in PBS) was added to each well of a streptavidin-coated 96-well microplate (BioBind Assembly strip, 1 × 8, streptavidin-coated, Thermo Fisher Scientific, Vantaa, Finland) and incubated at room temperature for 1 h. After three washes with 300 μl of PBS-T, each well was blocked with 200 μl of 2% PBS-M containing 5% DMSO for more than 30 min. After blocking, the liquid was discarded, and then 50 μl of 4% PBS-M containing 5% DMSO and 50 μl of culture supernatant containing soluble scFv were added. After a 1.5-h incubation, each well was washed, and 100 μl of an anti-myc-HRP antibody (1:1000 dilution in PBS; Miltenyi Biotec, Gladbach, Germany) was added. After a 1-h incubation, each well was washed, and 100 μl of ABTS Peroxidase Substrate (Kirkegaard and Perry Laboratories, Inc., Gaithersburg, MD) was added. After 20 min, the A_{405} was assessed using a microplate reader.

Sequence Analysis

Sequences of scFv were analyzed using BigDye Ver1.0 according to the manufacturer's protocol. Sequence primers used in the present study were LMB3 (5′-CAGGAAACAGCTATGAC-3′), Gene III leader (5′-GTGAAAAAATTATTATTCGCA-3′), and FDTSEQ1 (5′-GTCGTCTTTCCAGACGTTAGT-3′) for pMARXL and pFUSE-hIgG1-Fc2 FW(545–572) (5′-CTGAGATCACCGGCGAAGGAGGGCCACC-3′) and pFUSE-hIgG1-Fc2 RV(735–706) (5′-TGGGTTTTGGGGGGAAGAGGAAGACTGACG-3′) for pFX-hIgG1. The sequences were analyzed using the International ImMunoGeneTics Information System website (26).

Generation of scFv-hIgG and scFv Multimer

We constructed a derivative of pFUSE-hIgG-Fc2 (InvivoGen, San Diego, CA) that could express bivalent scFv with a constant region of human IgG to introduce the NotI site into the multicloning site. The mutation was inserted into the NotI site in the 3′-end of the ori sequence using a PrimeSTAR

Mutagenesis Basal kit with the primers pFUSE NotI mutation-sense (5′-ATCAGCGCCCGCAATAAAATATCTTTA-3′) and pFUSE NotI mutation-antisense (5′-TATTGCGGGCGC-TGATTTAAATGTTAAT-3′) according to the manufacturer's protocol. Next, we introduced a new multicloning site into the mutant vector. The vector was digested with EcoRV and BglII followed by column purification. The digested vector was ligated to annealed double-strand oligonucleotides (EcoRV/BglII pFUSEIghFC2 sense, 5′-ATCGGCCATGGTTTGGTACCTT-GCGGCCGCTA-3′; EcoRV/BglII pFUSEIghFC2 antisense, 5′-GATCTAGCGGCCGCAAGGTACCAAACCATGGCC-GAT-3′). The derivative of pFUSE-hIgG1-Fc2 was designated pFX-hIgG1. cDNA of VH and VL with a peptide linker of pMARXL was subcloned into pFX-hIgG1 via the NcoI-NotI site. For soluble expression of scFv-hIgG, 4 μg of the plasmid was transfected using Lipofectamine 2000 (Invitrogen) into 293T cells precultured on a 10-cm culture dish in DMEM supplemented with 10% FBS. After 4–5 h, the culture medium was replaced with fresh AIM V (Invitrogen) without serum. The supernatant was harvested and replaced with fresh AIM V at 24, 48, and 72 h after transfection. The collected supernatant was passed through a chromatography column with Protein G at 4 °C. The column was washed with 20 mM sodium phosphate (pH 7.0) and eluted by fraction (1 ml/fraction) with a total of 5 ml of 0.1 M glycine (pH 2.7) followed by immediate neutralization with 1/10 volume of Tris-HCl (pH 9.0). Fractions containing antibodies were assessed by SDS-PAGE with or without DDT to confirm that oxidized scFv-hIgG formed a dimer protein.

The multimer of scFv-hIgG1 (scFv multimer) was constructed as follows. Briefly, the Bir domain was introduced into the 3′-end of the hIgG1 Fc region by gene synthesis. Soluble expression and purification of the antibody protein were performed as described above. The antibody protein was biotinylated using the BirA enzyme and mixed with phycoerythrin-conjugated streptavidin to achieve a 1:4 molar ratio.

Surface Plasmon Resonance Analysis

Surface plasmon resonance analysis was performed using a ProteOn XPR36 (Bio-Rad) according to the protocol described by Nahshol *et al.* (27). Briefly, 1 μg/ml biotinylated monomer (HLA-A*02:01·PBF A2.2 peptide or HLA-A*02:01·HIV peptide) in PBS supplemented with 0.005% Tween 20 (PBST) was injected at 30 μl/min at 25 °C to be captured on a neutravidin-immobilized NLC sensor tip. Subsequently, serially diluted scFv-hIgG in PBST was injected at 50 μl/min at 25 °C. All binding sensorgrams were collected and analyzed using ProteOn Manager software (Bio-Rad).

Immunostaining and Flow Cytometry

Before immunostaining, T2 cells (5–10 × 10^5) were incubated in 200 μl of AIM V with each peptide at 50 μg/ml (PBF A2.2, HIV-A2, and CMV-A2) on a 96-well round bottom microculture plate at 26 °C overnight followed by 2-h incubation at 37 °C. For immunostaining, 5–10 × 10^6 target cells were seeded in a 96-well microculture plate and incubated with 50–100 μl of 10 μg/ml or 1 mg/ml scFv-hIgG or the supernatant of a hybridoma (BB7.2 or W6/32; purchased from American Type Culture Collection) on ice for 60–90 min. After two washes, the cells were incubated with 100 μl of anti-human IgG conjugated with Qdot655 (1:200 dilution; Invitrogen) or an FITC-conjugated rat anti-mouse IgG antibody (1:200 dilution; Kirkegaard and Perry Laboratories, Inc.) for 40 min. The cells were also stained with 50 μl of the scFv multimer (3 or 10 μg/ml) on ice for 60–90 min. After immunostaining, cells were washed and fixed with 200 μl of PBS with 0.5% formaldehyde and analyzed using FACS Array and CellQuest software (BD Biosciences). The reactivity of the antibodies was evaluated by the percent mean fluorescence intensity (%MFI) increase using the following calculation. %MFI increase = ((MFI of the samples − MFI of the negative control)/(MFI of the negative control)) × 100.

Inhibition Assay of Functional CTL Clone

CTL line 5A9 is an oligoclonal line containing HLA-A*02:01·PBF A2.2 peptide tetramer-positive cells that can recognize peptide PBF A2.2 in the context of HLA-A2 (20). After thawing the cryopreserved stock, cells were cultured in AIM V supplemented with 10% AB human serum and recombinant human IL-2 (200 units/ml; a kind gift from Takeda Pharmaceutical Company, Ltd., Osaka, Japan) in a 96-well microculture plate. On day 27, CTL 5A9 was stained with an anti-CD8-allophycocyanin APC antibody, HLA-A*02:01·PBF A2.2 tetramer-phycoerythrin, and HLA-A*02:01·HIV tetramer-FITC (negative control) (Medical & Biological Laboratories, Co., Ltd.) on ice for 30 min. After staining, the cells were incubated with anti-phycoerythrin magnetic beads (Miltenyi Biotech) followed by magnetic sorting of the tetramer-positive cells according to the manufacturer's protocol. U2OS cells (50,000 cells/well) were seeded in a 96-well flat bottom microculture plate. Next, the cells were preincubated with D12 scFv-hIgG1 or irrelevant D11 scFv-hIgG1 for 1 h at room temperature. Subsequently, sorted tetramer-positive cells (12,000 cells/well) or control medium without cells was added and cocultured for 20 h. The concentration of IFN-γ in the supernatant was analyzed using a human IFN-γ DuoSet ELISA Development kit (R&D Systems, Minneapolis, MN) according to the manufacturer's protocol.

RESULTS

Generation of a Naïve scFv Phage Display Library—We constructed an scFv phage display library with RNA extracted from human peripheral mononuclear cells of 31 naïve donors and two surgically resected tonsils on the new phagemid vector pMARXL (Fig. 1) using a total of 97 primers (supplemental Table S1). All 294 amplicons of VH, Vk, and Vl after primary PCR are shown in Fig. 2. The amplicons were used to introduce restriction enzyme sites by secondary PCR and subcloned into pMARXL. As a result, 16 initial sublibraries and 18 scFv sublibraries containing a total of 1.29 × 10^8 scFv clones were obtained (Table 1).

Three scFv Clones Recognized HLA-A2·Osteosarcoma Antigen PBF-derived Peptide Complex—We performed biopanning with a biotinylated HLA-A*02:01·PBF A2.2 peptide complex as the antigen and a rescued library phage. The ratios of output phage/input phage were 6.9 × 10^{-8} in the first round of biopanning, 6.2 × 10^{-7} in the second round, and 8.2 × 10^{-5} in the

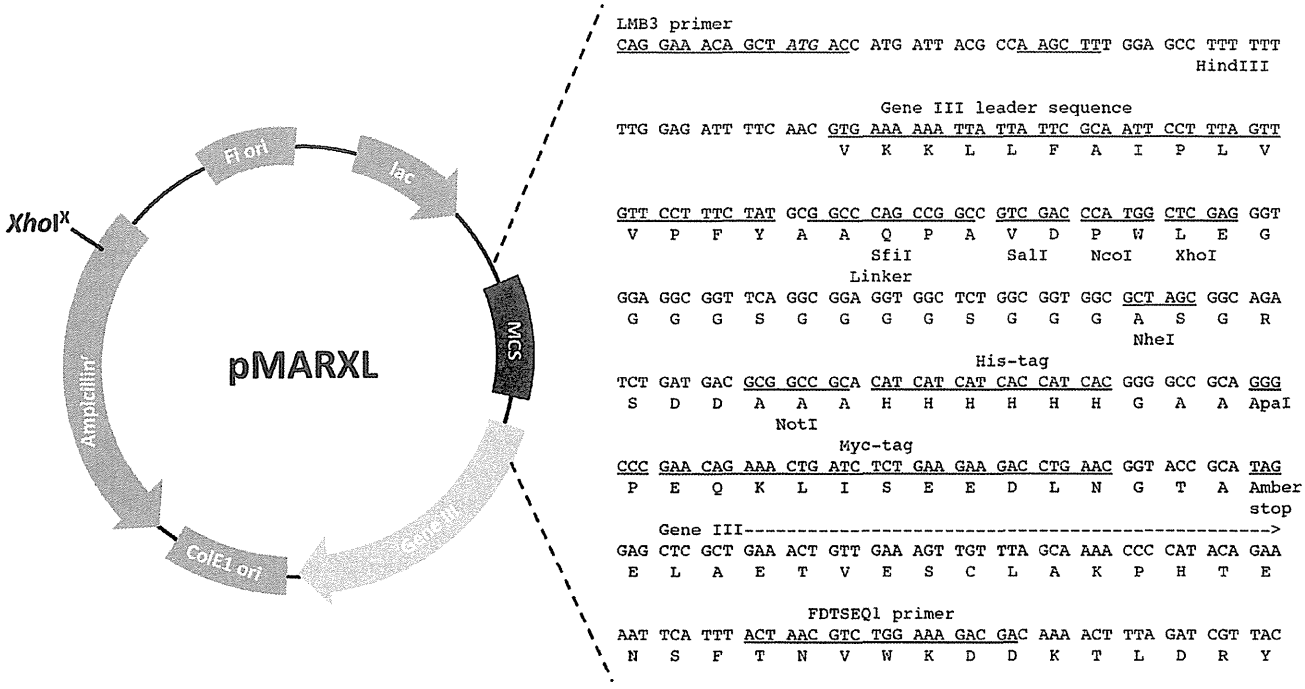

FIGURE 1. **Structure and sequence around the multicloning site of the phagemid vector pMARXL.**

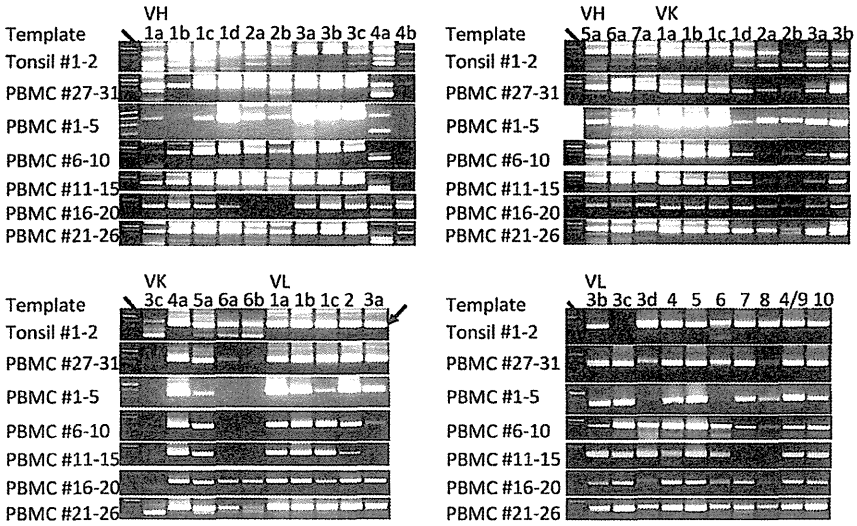

FIGURE 2. **Electrophoresis of amplified variable regions after primary PCR.** *Arrows* indicate the adequate amplicons (around 350 bp) containing variable regions.

third round (Fig. 3*A*). The gradual increase of the ratio indicated that adequate enrichment of specific phages was successfully achieved. Considering that the size of the libraries was 1.20×10^8 clones, a 10^{-20} order of enrichment efficiency was sufficient to isolate specific binders. After three rounds of biopanning, we screened the reactivities of 94 randomly selected scFv clones against the antigen by ELISA. As a result, we obtained three scFv clones (D12, G3, and H7) that were more highly reactive with the HLA-A*02:01·PBF A2.2 peptide complex than with the HLA-A*02:01·HIV peptide complex (Fig. 3*B*). Sequence analysis revealed that the three scFv clones had identical VH and VL (Fig. 3*C*).

*The scFv Clones Could React with Peptide PBF A2.2 Presented by HLA-A*02:01 on Antigen-presenting Cells with Strong Affinity*—Next, we constructed scFv-hIgG possessing bivalent scFv with the human IgG1 constant region and assessed whether the scFv clones could recognize peptide PBF A2.2 presented on the cell surface. D12 scFv-hIgG1 could successfully form an oxidized dimer (Fig. 4*A*.) The dimeric structures of the other clones were also confirmed (data not shown). We found that the three clones of scFv-hIgG could recognize T2 cells pulsed with peptide PBF A2.2 but not peptide HIV-A2 or peptide CMV-A2 (Fig. 4*B*). Monovalent scFv could not react with peptide-pulsed T2 cells (data not shown). We selected scFv

clone D12 as the representative clone for further analysis because the three clones contained an identical complementarity-determining region sequence and showed the same specificity. Kinetics analysis of protein interaction between scFv D12 and the HLA-A*02:01·PBF A2.2 peptide complex using surface plasmon resonance analysis showed the strong affinity of scFv D12 with the HLA-A*02:01·PBF A2.2 peptide complex (K_D = 1.53 × 10^{-9} M) (Fig. 4*C*). Simultaneously, D12 scFv-hIgG showed weak binding activity with the HLA-A*02:01·HIV peptide complex (Fig. 4*D*). Therefore, we assessed the cross-reactivity of D12 scFv-hIgG against the other biotinylated HLA-A*02:01·peptide complexes. We also confirmed that an HLA class I monoclonal antibody (supernatant of hybridoma W6/32) could highly react with all of the immobilized biotinylated complexes (data not shown). As shown in Fig. 4*E*, scFv D12-hIgG (5 and 0.5 μg/ml) reacted weakly with peptides NY-ESO-1, MPT51, and influenza M1. However, as shown in Fig. 4*B*, 10 μg/ml scFv D12-hIgG did not react with T2 cells pulsed with peptide HIV-A2 or with peptide CMV. Therefore, we considered that the cross-reactivity of scFv D12 was relatively low.

HLA-A2·PBF A2.2 Peptide Complex Was Firmly Expressed on the Surface of Osteosarcoma Cells—To assess whether scFv could detect peptide PBF A2.2 in the context of HLA-A2 presented on the sarcoma cell surface, we constructed a D12 scFv

TABLE 1

Scale of constructed libraries

*, prepared as the "additional libraries" described under "Experimental Procedures."

Scale of initial libraries of heavy and light chains.					
Heavy chain		Kappa chain		Lambda chain	
VH1	4.29×10^7	Vk1	0.35×10^7	Vl1	0.51×10^7
VH2	0.56×10^7	Vk2	0.12×10^7	Vl2	0.33×10^7
VH3	1.44×10^7	Vk3	0.11×10^7	Vl3	0.30×10^7
VH4	0.48×10^7	Vk4	0.52×10^7		
VH5	1.43×10^7	Vk5	0.60×10^7		
VH6	1.09×10^7	Vk6	0.40×10^7		
VH7	0.50×10^7				
Total	9.80×10^7		2.10×10^7		1.14×10^7

Scale of final scFv libraries.					
Heavy and kappa chains		Heavy and lambda chains		Heavy and specific light chains	
VH1k	1.65×10^7	VH1l	0.87×10^7	VH3-Vk1	0.73×10^7
VH2k	0.73×10^7	VH2l	0.33×10^7	VH3-Vl2	0.21×10^7
VH3k	0.31×10^7	VH3l	0.36×10^7		
VH4k	0.15×10^7	VH4l	0.15×10^7		
VH5k	0.49×10^7	VH5l	0.54×10^7	VH3-Vk1*	1.79×10^7
VH6k	2.13×10^7	VH6l	1.02×10^7	VH3-Vl6*	0.64×10^7
VH7k	0.47×10^7	VH7l	0.28×10^7		
Total	5.92×10^7		3.56×10^7		3.37×10^7

A

Panning round	Input phage (pfu)	Output phage (pfu)	ratio
1st	1.6×10^{11}	1.1×10^4	6.9×10^{-8}
2nd	7.7×10^{12}	4.0×10^6	6.2×10^{-7}
3rd	1.1×10^{13}	9.0×10^8	8.2×10^{-5}

B

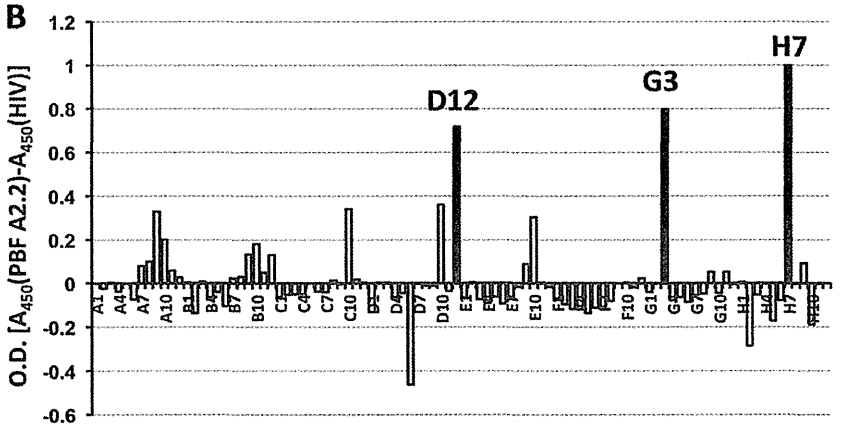

C

Clone	Chain	V-GENE	J-GENE	D-GENE	CDR3
G3	VH	IGHV3-43*02	IGHJ3*02	IGHD1-14*01	CVKGLTYYRDAFDIW
	VL	IGKV1-5*03	IGKJ2*01		CQQYNSYSYTF
H7	VH	IGHV3-43*02	IGHJ3*02	IGHD1-14*01	CVKGLTYYRDAFDIW
	VL	IGKV1-5*03	IGKJ2*01		CQQYNSYSYTF
D12	VH	IGHV3-43*02	IGHJ3*02	IGHD1-14*01	CVKGLTYYRDAFDIW
	VL	IGKV1-5*03	IGKJ2*01		CQQYNSYSYTF

FIGURE 3. **Three scFv clones recognized HLA-A2·osteosarcoma antigen PBF-derived peptide complex.** *A*, input/output ratios of phage particles. *B*, ELISA screening of the specific binders of 94 scFv clones reacting with biotinylated HLA-A*02:01·PBF A2.2 peptide complex. *C*, sequence analysis of complementarity-determining region 3 (*CDR3*) region of scFv clones.

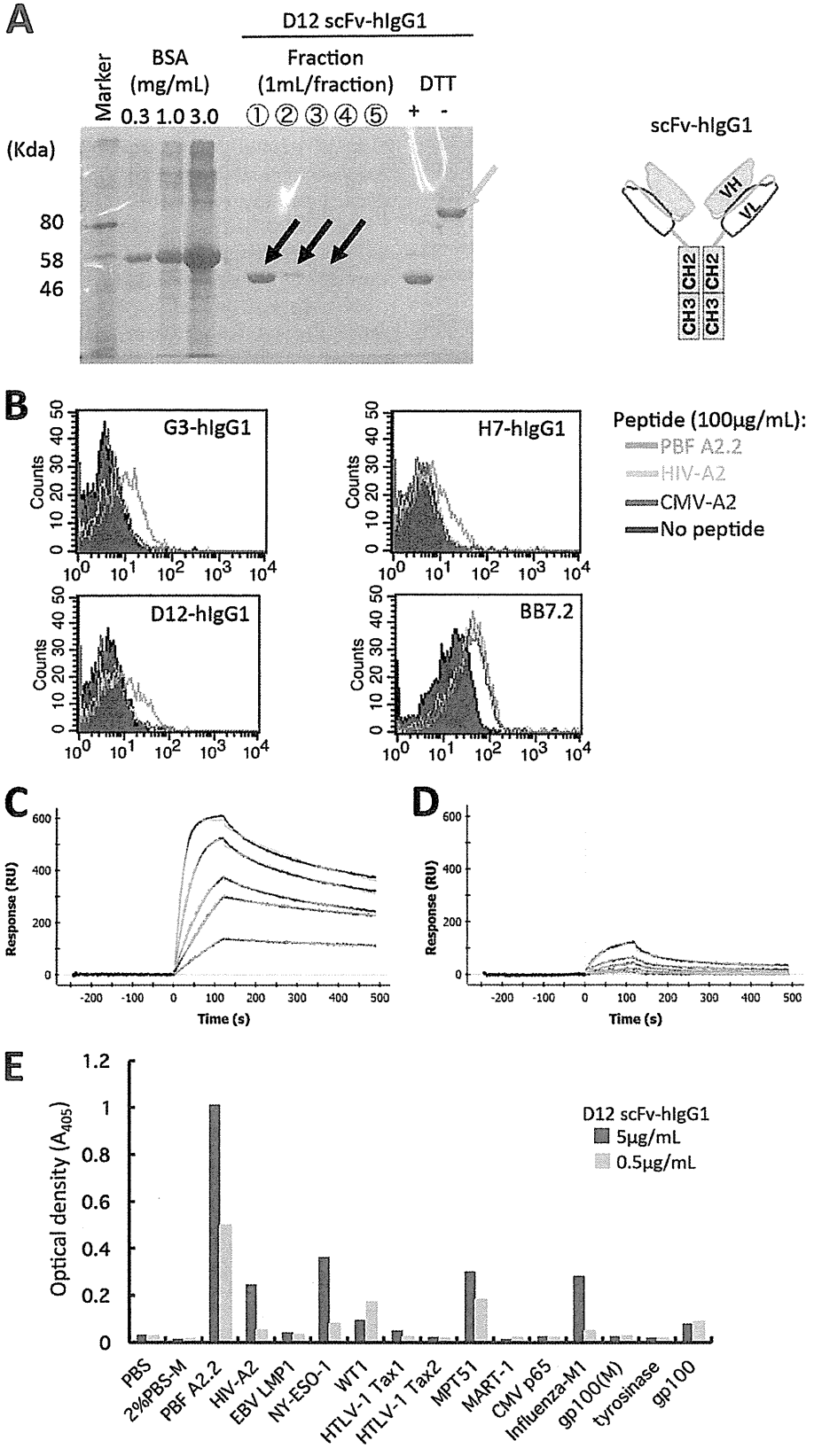
A
D12 scFv-hIgG1
Marker
BSA (mg/mL)
0.3 1.0 3.0
Fraction (1mL/fraction)
① ② ③ ④ ⑤
DTT
+ -
(Kda)
80
58
46
scFv-hIgG1
VH
VL
CH2
CH2
CH3
CH3
B
G3-hIgG1
H7-hIgG1
D12-hIgG1
BB7.2
Counts
Peptide (100μg/mL):
PBF A2.2
HIV-A2
CMV-A2
No peptide
C
D
Response (RU)
Time (s)
E
Optical density (A_{405})
D12 scFv-hIgG1
5μg/mL
0.5μg/mL
PBS
2%PBS-M
PBF A2.2
HIV-A2
EBV LMP1
NY-ESO-1
WT1
HTLV-1 Tax1
HTLV-1 Tax2
MPT51
MART-1
CMV p65
Influenza-M1
gp100(M)
tyrosinase
gp100

multimer (Fig. 5*A*) because bivalent scFv (D12 scFv-hIgG1) failed to react with HLA-A2-positive sarcoma cells (data not shown). The D12 scFv multimer (10 μg/ml) reacted highly with T2 cells pulsed with peptide PBF A2.2 and did not react with the cells pulsed with peptide CMV. Conversely, the multimer reacted with the cells pulsed with peptide HIV-A2 at a concentration of 100 μg/ml. These findings suggested that the low cross-reactivity against peptide HIV-A2 of D12 scFv was enhanced by multimer formation. Therefore, we titrated the reactivity of the multimer by calculation of the MFI against T2 cells pulsed with the peptides at various concentrations between 5 fg/ml and 50 μg/ml (Fig. 5*B* and Table 2). Although the multimer (3 μg/ml) also reacted with peptide HIV-A2 (pulsed at 50 μg/ml), its reactivity against the peptide was hardly detected at the concentration of 50 ng/ml (Fig. 5*B*). Conversely, the reactivity against peptide PBF A2.2 was preserved at the lower concentration of 500 pg/ml. The affinity of the multimer against peptide PBF A2.2 was estimated to be 100-fold higher than for peptide HIV-A2. In addition, we considered that a 20.0% MFI increase might be the threshold of the reactivity of the D12 scFv multimer. Next, six sarcoma cell lines and one primary culture of osteosarcoma were stained with the D12 scFv multimer (Fig. 5*C*). The reactivity of the multimer was graded as follows: strong (≥100% MFI increase), weak (≥20% but <100% MFI increase), and none (<20% MFI increase). In the context of HLA-A2, peptide PBF A2.2 was strongly detected on U2OS (A*02:01), HOS (A*02:11), and Saos-2 (A*02:01); weakly detected on KIKU (A*02:06); and not detected on HLA-A2-negative OS2000 and MFH2003 cells. In addition, peptide PBF A2.2 was also weakly detected on primary cultured osteosarcoma, which highly expressed HLA-A*02:01. These findings suggested that the D12 scFv multimer could react with peptide PBF A2.2 presented by HLA-A2. Simultaneously, the HLA-A2·PBF A2.2 peptide complex was expressed on osteosarcoma cells at various levels.

*D12 scFv Showed Similar Specificity with Natural CTL Recognizing HLA-A*02:01·PBF A2.2 Peptide Complex*—To assess the similarity of specific responses against the HLA-A2·PBF A2.2 peptide complex between natural TCR and scFv, we performed inhibition assay of the CTL-mediated response against PBF A2.2. The frozen oligoclonal CTL line 5A9 was thawed and cultured followed by the selection of tetramer-positive cells using magnetic beads (Fig. 6*A*). The CTL response against HLA-A*02:01-positive osteosarcoma cell line U2OS was assessed by ELISA (Fig. 6*B*). Next, U2OS cells were preincubated with D12 scFv-hIgG1 or irrelevant D11 scFv-hIgG1 and cocultured with tetramer-positive CTL 5A9. As a result, partial inhibition (~20%) of the scFv-mediated CTL response was observed. These findings suggested that scFv had specificity similar to that of functional TCR directed to the cognate antigen.

DISCUSSION

In the present study, we constructed a naïve scFv phage display library and isolated scFv clone D12, which reacted with the HLA-A*02:01·PBF A2.2 peptide complex with strong affinity. Bivalent and multivalent scFv D12 could react with peptide-pulsed T2 cells and HLA-A2-positive sarcoma cell lines, and D12 scFv could inhibit the natural TCR-mediated CTL response. These findings suggested that the D12 scFv clone had specificity mimicking that of the natural TCR against the HLA-A*02:01·PBF A2.2 peptide complex. Simultaneously, the HLA-A2·PBF A2.2 peptide complex was strongly and naturally expressed on osteosarcoma cells.

Generation of antibodies recognizing HLA·peptide complexes derived from tumor-associated antigens has been reported mainly in the field of melanoma (28). Development of such antibodies against HLA·peptide complexes is significant because assessment of the expression status of HLA·vaccine peptide complexes is important to select candidate patients and predict the efficacy of peptide-based immunotherapy. Moreover, antibodies mimicking TCR with high specificity and affinity could serve as sources of antibody-based therapy and chimeric antigenic receptors. However, the generation of antibodies that react with HLA·peptide complexes is still much more difficult than generation of those that react with the other proteins. This might be because the construction of antibody phage display libraries from naïve donors with sufficient quality and diversity is very hard and requires intensive laboratory work.

Generally, the amount of a single peptide presented by HLA class I molecules is very small. Purbhoo *et al.* reported that the HLA-A2·NY-ESO-1(157–165) peptide complex presented on melanoma cells ranged from 10 to 50 copies per cell as assessed by soluble high affinity engineered TCR (29). A similarly copy number of the HLA-A*02:01·gp100 peptide complex was barely detected by FACS but could be recognized by CTL (30). In the present study, strong expression levels of the HLA-A*02:01·PBF A2.2 peptide complex were detected on U2OS, HOS, and Saos-2 cells, but only weak levels were detected on KIKU and primary OS. These results suggested that the HLA-A2·PBF A2.2 peptide complex was naturally presented on osteosarcoma cells as in melanoma and might be a good candidate for peptide-based immunotherapy. Obviously, the possibility of the cross-reactivity of scFv clone D12 against the other antigens could not be completely ruled out. Indeed, the D12 scFv multimer mildly reacted with HIV-A2 peptide-pulsed T2 cells and other HLA·peptide complex monomers (NY-ESO-1, MPT51, and influenza M1). Among these peptides, no similar amino acid sequence was observed, excluding the anchor residues of HLA-A2 protein, leucine (Leu) at position 2 and valine (Val) at the C terminus (31). Therefore, the cross-reactivity might not depend on the epitope sequence but on some conformational

FIGURE 4. **The scFv clones could react with peptide PBF A2.2 presented by HLA-A*02:01 on antigen-presenting cells with strong affinity.** *A*, soluble fractions of D12 scFv-hIgG1 after purification with Protein G are visualized by SDS-PAGE. The reduced monomer (*black arrows*) and oxidized dimer of scFv-hIgG (*red arrow*) of fraction 1 are indicated. *B*, FACS analysis of scFv-hIgG1. T2 cells were pulsed with the indicated peptides and stained with each scFv-hIgG1 at a concentration of 10 μg/ml. BB7.2 was used to detect expression of HLA-A2 molecules. *C* and *D*, surface plasmon resonance analysis. Biotinylated HLA-A*02:01·PBF A2.2 peptide complex (*C*) or HLA-A*02:01·HIV-A2 peptide complex (*D*) was immobilized on the sensor tip as the target. Serially diluted D12 scFv-hIgG1 was used as the analyte as described under "Experimental Procedures." *E*, ELISA screening of the reactivity of D12 scFv-hIgG against various biotinylated HLA-A*02:01·peptide complexes. *RU*, response units; *EBV*, Epstein-Barr virus; *HTLV-1*, human T-lymphotropic virus type I.